Beyond neuromuscular activity: botulinum toxin type A exerts direct central action on spinal control of movement

Šoštarić, Petra; Matić, Magdalena; Nemanić, Dalia; Lučev Vasić, Željka; Cifrek, Mario; Pirazzini, Marco; Matak, Ivica

Source / Izvornik: **European Journal of Pharmacology, 2024, 962**

Journal article, Accepted version
Rad u časopisu, Završna verzija rukopisa prihvaćena za objavljivanje (postprint)

https://doi.org/10.1016/j.ejphar.2023.176242

Permanent link / Trajna poveznica: https://urn.nsk.hr/urn:nbn:hr:105:410200

Beyond neuromuscular activity: botulinum toxin type A exerts direct central action on spinal control of movement

Petra Šoštarić[1], Magdalena Matić[1,2], Dalia Nemanić[3], Željka Lučev Vasić[4], Mario Cifrek[4], Marco Pirazzini[5,6], Ivica Matak[1]*

1 Laboratory of Molecular Neuropharmacology, Department of Pharmacology and Croatian Institute of Brain Research, University of Zagreb School of Medicine, Šalata 11, 10000 Zagreb, Croatia

2 Division of Neurobiology, Department of Neurology, Medical University of Innsbruck, Innsbruck, Austria

3 Department of Pharmacology, Faculty of Pharmacy and Biochemistry, University of Zagreb, Domagojeva 2, 10 000 Zagreb, Croatia

4 University of Zagreb, Faculty of Electrical Engineering and Computing, Zagreb, Croatia

5 Department of Biomedical Sciences, University of Padova, via Ugo Bassi 58/B 35131, Padova, Italy

6 Interdepartmental Research Center of Myology CIR-Myo, University of Padova, Via Ugo Bassi 58/B, 35131 Padova, Italy

*Correspondence: ivica.matak@mef.hr; Tel.: 0038514590198

Type of article: Original research article

ABSTRACT

Overt muscle activity and impaired spinal locomotor control hampering coordinated movement is a hallmark of spasticity and movement disorders like dystonia. While botulinum toxin A (BoNT-A) standard therapy alleviates mentioned symptoms presumably due to its peripheral neuromuscular actions alone, the aim of present study was to examine for the first time the toxin's trans-synaptic activity within central circuits that govern the skilled movement. The rat hindlimb motor pools were targeted by BoNT-A intrasciatic bilateral injection (2 U per nerve), while its trans-synaptic action on premotor inputs was blocked by intrathecal BoNT-A-neutralising antitoxin (5 i.u.). Effects of BoNT-A on coordinated and high intensity motor tasks (rotarod, beamwalk swimming), and localised muscle weakness (digit abduction, gait ability) were followed until their substantial recovery by day 56 post BoNT-A. Later, (day 62-77) the BoNT-A effects were examined in unilateral calf muscle spasm evoked by tetanus toxin (TeNT, 1.5 ng). In comparison to peripheral effect alone, combined peripheral and central trans-synaptic BoNT-A action induced a more prominent and longer impairment of different motor tasks, as well as the localised muscle weakness. After near-complete recovery of motor functions, the BoNT-A maintained the ability to reduce the experimental calf spasm evoked by tetanus toxin (TeNT 1.5 ng, day 62) without altering the monosynaptic reflex excitability. These results indicate that, in addition to muscle terminals, BoNT-A-mediated control of hyperactive muscle activity in movement disorders and spasticity may involve the spinal premotor inputs and central circuits participating in the skilled locomotor performance.

Key words: botulinum toxin type A; motor control; axonal transport; spinal cord; trans-synaptic effect

1. Introduction

Used as a pharmaceutical-grade purified low dose preparation, botulinum neurotoxin serotype A (BoNT-A) is employed in various disorders involving motor, autonomic and sensory nerve hyperactivity (Rosseto and Montecucco, 2019; Jankovic 2017; Anandan and Jankovic 2021). It poisons the presynaptic nerve terminals for several months by first binding to

polysialoganglioside and synaptic vesicle 2 (SV2) protein, followed by endocytotic entry into recycled synaptic vesicles. Upon vesicle acidification, the toxin translocates its 50 kDa neurotoxic light chain into the presynaptic cytosol, and cleaves synaptosomal-associated protein of 25 kDa (SNAP-25) (Schiavo et al., 1993; Rossetto et al., 2014) with consequent long-term blockage of the Ca^{2+}-triggered release of ACh and other neurotransmitters Gundersen 1980; Pirazzini et al., 2017). In focal dystonias and spasticity, its therapeutic benefits have been commonly attributed to local neuromuscular paralysis of injected muscles, in turn, leading to indirect central plastic changes (Rosales and Dressler, 2010). However, mounting data point to a direct central interaction with sensory and motor systems (Matak and Lacković 2014; Ramachandran and Yaksh, 2014; Ramirez-Castaneda et al., 2013; Mazzocchio and Caleo, 2015). The BoNT-A may normalise the spastic co-contraction of agonists and antagonists and recover the reciprocal inhibition in uninjected muscles, possibly by influencing the recurrent inhibition at a synapse between motoneuronal collaterals and Renshaw interneurons (Hallett 2018; Gracies 2004; Matak et al., 2016; Vinti et al., 2012; Marchand-Pauvert et al., 2013; Aymard et al., 2013; Caleo and Mazzocchio, 2018; Weise et al., 2019). Peripherally injected BoNT-A is axonally transported to spinal cord and brainstem nuclei (Antonucci et al., 2008; Matak et al., 2012; Restani et al.,2012; Koizumi et al., 2014; Caleo et al., 2018). Furthermore, its central antispastic effect has been reported in rat focal muscle hypertonia induced by tetanus toxin (TeNT) (Matak 2020; Šoštarić et al., 2022), a neurotoxin that blocks the inhibitory transmission (Brooks et al.,1957; Megighian et al., 2021). The BoNT-A central trans-synaptic traffic was found to be necessary for its antispastic effect when local muscular effects of BoNT-A are minimised or start to recover (Matak 2020; Šoštarić et al., 2022). Other motor consequences of BoNT-A trans-synaptic transport in ventral horn are, up to now, unknown. Spinal premotor inputs regulate the precise activation of different muscle groups during normal locomotion (Laliberte et al., 2019). In dystonia and spasticity, spinal locomotor circuits produce altered patterns of motor pool activation leading to sustained or intermittent muscular hyperactivity (Liu et al., 2015; Bellardita et al., 2017; Pocratsky et al., 2023). Building on our previous research that demonstrated the BoNT-A axonal transport and

transcytosis (Caleo et al., 2018; Matak 2020; Šoštarić et al., 2022), we hypothesised that spinal synapses sensitive to BoNT-A may belong to premotor inputs regulating the precise activation of different muscle groups during locomotion.

To examine this hypothesis, we studied the effect of BoNT-A in the motor system by targeting the bilateral lower leg and hind-paw motor pools in adult rats. We employed direct toxin injections into the sciatic nerves (i.n.) rather than into multiple hindlimb muscles. This enabled a slower-onset toxin effect at the NMJ due to anterograde transport resulting in milder weakness, however with ongoing muscle atrophy, and a central enzymatic action similar to the one seen after i.m. BoNT-A in previous studies (Matak 2020; Šoštarić et al., 2022). We further characterised the effect of unopposed vs opposed BoNT-A spinal trans-synaptic action on the motor performance by blocking its trans-synaptic transport with intrathecal BoNT-A-neutralising antitoxin. Then, its motor effects were regularly assessed by different behavioural tests up to 56 days after BoNT-A injection. Later, in the same animals we examined BoNT-A central action on TeNT-evoked spasm and exaggerated monosynaptic H reflex and, at the end of experiment, analysed the localization of the toxin enzymatic activity in relation to synaptic markers and known toxin acceptors.

2. Material and methods

2.1. Animals

Adult male Wistar Han rats (University of Zagreb School of Medicine, Croatia), 6 months old and weighing 494 ± 9 g at the beginning of the experiment, were used. Three rats per home cage supplied with cardboard play tunnel enrichment were kept under a 12 hour light/dark cycle and *ad libitum* access to food and water. All procedures involving animals and animal care were carried out in accordance with the European Union Directive (2010/63/EU), the ARRIVE guidelines 2.0: Updated guidelines for reporting animal research (Percie et al., 2020) and approved by the institutional review board (University of Zagreb School of Medicine) and Croatian Ministry of Agriculture ethical committees (permit no. EP 229/2019). The adult

rats of single sex (male) were chosen to achieve more uniform weight and dosing that is not affected by differences related to sexual dimorphism e.g. muscle size, total weight of rats, length of the nerves, as well as to minimise any possible systemic effect of the injected BoNT-A (lower dosage/body weight ratio).

2.2. Drugs

Following drugs were used: lyophilized BoNT-A (INN: clostridium botulinum type A neurotoxin complex, Allergan, Irvine, CA, USA) was reconstituted in physiological saline. Lyophilized polyclonal equine IgG-based BoNT-A antitoxin (NIBSC code 14/174, National Institute for Biological Standards and Control, Potters Bar, United Kingdom; a kind gift from Dr. Thea Sesardic), validated by Li et al. (2012) , was reconstituted in 0.9% sterile saline to obtain1000 international units (iu)/ml concentration (single i.u. can neutralise 10 000 mouse LD_{50} doses of BoNT-A), and further kept in ultrafreezer, until use. Lyophilized TeNT (Sigma Aldrich, St Louis, MO, USA, Cat. No T3194) was reconstituted in saline vehicle containing 2% bovine serum albumin (BSA) (Sigma Aldrich), kept in concentrated aliquots at −80°C, and further diluted with vehicle containing 2% BSA to the necessary volume for i.m. injections.

2.3. Pharmacological treatment

Animals were assigned randomly into different experimental groups by using block randomisation. For bilateral i.n. injection of BoNT-A or saline, the rats were deeply anaesthetised with a mixture of ketamine (Ketamidor® 10%, Richter Pharma AG, Wels, Austria; 70 mg/kg i.p.) and xylazine (Xylased® Bio, Bioveta, Ivanovice na Hané, Czech Republic; 7 mg/kg i.p.). The fur of the rat thigh was clipped and disinfected with 70% ethanol, and then a lateral skin incision (1.5 cm) at mid-femoral level was made. The sciatic nerve was exposed by blunt dissection through the thigh muscles and exposed with curved forceps. The BoNT-A injection into the nerve trunk was performed with a 0-10 µl Hamilton syringe needle (Cat. No. #701, Hamilton, Bonadouz, Switzerland) as previously described (Bach-Rojecky and Lacković 2009). The nerve was left in place for three minutes following the treatment and

retracted to its natural position by leg extension, followed by skin suturing. Then, the operation and injection procedure were repeated on the contralateral limb (fig 1).

The next day (24 h post BoNT-A), animals were injected i.t. into the spinal canal at level of cauda equina with equine serum containing 5 iu of BoNT-A-neutralizing equine antitoxin (National Institute for Biological Standards and Control, NIBSC code 14/174, Potters Bar, United Kingdom,) or horse serum administered as a control treatment for equine serum (Gibco, ThermoFisher Scientific, Waltham, MA, USA). Prior to i.t. treatment, both neutralising antiserum solution and control horse serum (5 µl each per animal) were diluted with equal amount of saline to obtain the total volume of 10 µl per animal. The i.t. administration was performed under isoflurane anaesthesia (5% induction, 2 % maintenance) by 28G x ½'' tip of 0.5 ml tuberculin syringe inserted between the lumbar vertebrae (L4-L6) into vertebral canal at the level of cauda equina, as previously described (Matak 2020; Šoštarić et al., 2022). Brief, sudden movement of hind limb or tail was monitored as a confirmation of successful targeting of lumbar spinal canal.

Tetanus toxin (TeNT; Sigma Aldrich, Cat. No T3194) diluted in saline vehicle containing 2% BSA was administered on day 62 after BoNT-A into the calf to induce local hindlimb spasticity. The rats were i.m. injected under anaesthesia with 10 µL of neurotoxin divided into 2 injection sites (5 µL each site) i.m. into the lateral and medial belly of the right gastrocnemius by employing 10 µL Hamilton syringe. The 1.5 ng TeNT dose was chosen based on previously used non-systemic doses (Matak 2020; Šoštarić et al., Matthews et al.,2014).

Figure 1.

2.4. Behavioural motor tests

Experimenters were blinded to the animal treatment during performance of i.n. and i.t. treatments and measurements. All motor tests were conducted during the day at similar time periods (from 9 a.m. to 2 p.m.).

2.4.1. Narrow beam walking

Rats were trained to cross an elevated rectangular horizontal beam (2.5 cm × 2.5 cm × 100 cm) connecting a rectangular platform (10 cm × 10 cm) exposed to lamp light on one side and an enclosed “safe” dark platform (25 cm × 25 cm × 25 cm, 10 cm × 10 cm entrance) on the other side, as previously described (Šoštarić et al., 2022; Carter et al.,2001). The latency was defined as the transit time between the markings placed at 10 cm from both ends of the beam (80 cm total distance), with the average calculated from two successful trials per single measurement (Matak 2020). Animals were pre-trained daily during the week preceding the BoNT-A i.n. treatment to cross the bar swiftly without stumbling, stopping or falling.

2.4.2. Rotarod test

The animals were placed on a rotarod device rotating at constant rate (13 r.p.m.). The time that the animal spent on the rotating bar (8-cm diameter) before falling was then measured, with the maximal trial duration set to 180 s. Animals were pre trained to easily maintain the balance for 3 minutes before the toxin treatment. The latency value was calculated based on two trials per a single measurement session, with at least 20 min resting period between the trials.

2.4.3. Swimming performance

Individual rats were placed inside the circular swimming pool filled with water (180 cm diameter, water depth 30 cm, temperature 24 ˚C), and observed with a wide-angle video camera (Basler AG, Basler, Ahrensburg, Germany) mounted above. The swimming mean and maximal velocity during a time period of 120 s per trial were assessed by video analysis software (Noldus Ethovision XT ver. 11.5; Noldus, Wageningen, Netherlands) monitoring the animal’s body centre position every 0.133 s (7.5 Hz). To exclude the low values when animals did not swim (e.g. during passive floating), or erroneously high values, only the velocities between 10 to 100 cm/s were considered. The parameters were calculated based on two trials per measurement session with at least 30 min resting period between the trials. The animals

exhibit an innate ability to swim and did not require pre-training prior to the baseline measurement.

2.4.4. Digit abduction score (DAS)

To assess the toe-spreading reflex impairment, animals were gently grasped around the waist and lifted, and the toe spreading was quantified with scores based on toe abduction defined as 0 = separation of all toes; 1 = separation of four toes; 2 = separation of three toes; 3 = separation of two toes; and 4 = no toe separation (Broide et al., 2013). The DAS value was based on the average score of both hind-limbs and by the two independent observers unaware of the animal treatment.

2.4.5. Gait ability test

The appearance of rat hind paws and leg use during gait and climbing, indicative of lower leg muscle weakness, was assessed by the gait ability score as previously explained in details (Brent et al., 2020; Warner et al., 2006). The total score ranging from 0-10 was based on the sum of scores from five different parameters: 1) hindlimb abduction during suspension by the animal's tail; the hind paw appearance that evaluated the weight bearing by interdigital paw pad and toes (normal) vs the use of heel (abnormal) during 2) sitting on the ground; 3) bipedal stance while leaning against the cage side, 4) while walking on a slope, 5) gripping with toes and propulsion by both toes and interdigital paw pad during climbing on the inclined mesh floor. Each set of observations was scored with scale of individual parameter ranging from disabled (0) to normal (2) (e.g. markedly arch-like appearance of the hind-paw in contact with the ground scored as 0; intermediate foot sole arching with partially curled toes scored 1, no arching and normal foot appearance with toe extension and interdigital paw pad in contact with the ground scored as 2). The gait ability value from single measurement was based on the average score of both hind-limbs and by the two independent observers unaware of the animal treatment.

2.4.6. Resistance to passive ankle flexion

Digital zeroed kitchen scale with a plastic platform attached on its surface (dimensions in cm: 1.5 × 4 × 4) was used for assessing the passive ankle flexion resistance. Animals were lifted by the examiner's hand and the ankle joint was flexed by pressing the hind paw interdigital pad area against the platform. The dorsiflexion of TeNT-treated spastic hind-limb was performed until > 90° tibiotarsal angle was reached, after which the pressure was slightly relieved until the tibiotarsal angle returned to 90°. At that point the resistance value in grams (g) was noted and the average of two measurements per session was calculated (Matak 2020; Šoštarić et al., 2022).

2.4.7. Basso Beattie Bresnahan locomotor scale

The appearance of TeNT-treated hind limb and its use during gait was examined by employing the Basso Beattie Bresnahan (BBB) locomotor rating scale. The BBB score range (0-21) consists of a combination of defined elements describing the hind limb joint movement, paw placement, weight support, forelimb-hindlimb coordination, paw position during locomotion, toe clearance during limb advancement, tail position, and trunk stability during gait (Basso et al., 1995). The rats were video-recorded while walking across a table to return to their home cage opened in level with the table surface, as previously described (Šoštarić et al., 2022). Two observers unaware of the animal treatment assessed the BBB score from coded video footage, and the mean of their independent scoring counted as a single measurement. Only the right hind limb injected with TeNT was used to assign the score, while contralateral non-spastic limb served as a reference for normal range of motion of joints.

2.4.8. Measurement of lower leg muscle atrophy

Changes of the lower leg width were used to assess the muscle atrophy throughout the experiment. The approximate cross section area of the lower leg was modelled as ellipse defined by the mediolateral (ML) and dorsoventral (DV) calf diameter at its widest mid-belly part (DV × ML × π/4) measured by calliper (Šoštarić et al., 2022). The values representing single animal measurements were calculated as average value obtained from both legs. The calf diameters were measured prior to the treatment and at different experimental points after

i.n. BoNT-A. At the end of the experiment, the gastrocnemius and soleus muscles from saline and fixative-perfused animals were dissected and their weights measured on a laboratory scale. The cross section area and weight values were based on the average score of both hind-limbs.

2.5. Electromyography (EMG)

The CMAP (M-wave) and monosynaptic reflex (Hoffmann's reflex or H-reflex) were recorded from right gastrocnemius muscle on day 62 after BoNT-A treatment (prior to TeNT treatment) and on days 8 and 15 after TeNT. The EMG measurements were performed under general anaesthesia with ketamine/xylazine (70/7 mg/kg i.p.). Rats were placed in a prone position inside a narrow wooden box slightly elevated from the ground (5 cm) with tail and hind limbs protruding out. The stimulating 29 G stainless steel needle electrodes (Cat. #. MLA1203, AD Instruments, Oxford, UK) were inserted s.c. over the sciatic notch and mid-thigh femur. The recording needle electrode was inserted perpendicularly into the lateral gastrocnemius head belly to the depth that just penetrated the skin and entered the muscle. The reference electrode was inserted s.c. over the lateral malleolus, and the ground electrode was placed subcutaneously into the thoracolumbar back. Both stimulation and recording electrodes were connected to the two-channel extracellular amplifier (EXT-02B, NPI electronic GmbH, Germany) via two headstages. The recording of muscle potentials was performed in differential mode. Analog signals obtained from the amplifier were digitised via data acquisition unit (Micro1401-4, CED, UK) and then fed to a PC for both online visualisation and offline analysis using Spike2 software version 10 (CED, Cambridge, UK). The PC-controlled transistor–transistor logic signal pulses fed via the same acquisition unit switched one of the amplifier channels from recording to stimulation mode, and activated the stimulus isolator (ISO 01 D, NPI electronic, GmbH, Germany) to generate the 200 μs rectangular voltage pulses that were, in turn, redirected via amplifier and headstage to the stimulating electrodes. From the stimulated sciatic nerve trunk, orthodromic and antidromic depolarization waves travelling via myelinated fibres generated a short latency CMAP or M wave, and a delayed Hoffmann's or

H-reflex muscle activation evoked by monosynaptic activation of motoneurons by electrically stimulated Ia afferents. The maximal peak-to-peak amplitudes of M wave and H-reflex in mV (M_{max} and H_{max}) were measured by stimulation with increasing voltages. The H-reflex was confirmed by eliciting the rate-dependent depression by repeated pulse train (10 x, 4 Hz, delivered at voltage that elicits H_{max}). Mean H_{max} and M_{max} were determined based on 3 independent waveforms generated with at least 5 s delay between the pulses (Matthews et al.,2014; Ho and Waite, 2002).

2.6. Immunohistochemistry

At the end of the experiment, animals were deeply anaesthetised with ketamine/xylazine and killed by transcardial perfusion with physiological saline (400-500 ml), followed by 250 ml 4% paraformaldehyde fixative. Left and right gastrocnemius, soleus and spinal cord were excised. All tissues were post-fixed and cryoprotected overnight in 15 % sucrose with fixative, and the next day transferred to 30 % sucrose in 1 x phosphate buffered saline (PBS). After the tissue sank it was further stored at -80 ºC. Spinal cords were cut in cryostat at 35 µm thick slices and transferred to free floating wells for immunohistochemistry, while muscles were cut at 20 µm slice thickness and immediately transferred to glass adhesion slides (Super Frost Plus Gold, Thermo Scientific, Waltham, USA), kept at -20 ºC. Spinal cord slices were washed with PBS and incubated with 3 % H_2O_2 for inhibition of endogenous peroxidase. Then the slices were washed again, followed by blocking with 10 % normal goat serum (NGS), and incubated overnight at room temperature with non-affinity purified rabbit polyclonal antibody recognizing the BoNT-A-cleaved SNAP-25 fragment ($SNAP\text{-}25_{197}$; 1:8000, National Institute for Biological Standards and Control, Potters Bar, UK) validated in previous studies (Ekong et al., 1997; Jones et al., 2008). Next day the tissue was incubated with HRP-polyconjugated (polyHRP) goat anti rabbit secondary antibody (Tyramide SuperBoost Kit B40923/Invitrogen), and then with tyramide Atto-488 HRP substrate prepared as described previously (Homolak et al., 2022), for 10 minutes. After that, the slices were washed, mounted on glass slides and coverslipped with anti-fading agent. For colocalization

analyses the slices were incubated overnight with different primary antibodies (Table1.). After overnight incubation, the slices were washed and then incubated for 2 hours with Alexa 555 secondary antibody (Table1.) diluted in 1% NGS and PBS with 0.25% triton X-100 (PBST), and later mounted on glass as previously stated. The fluorescent microphotographs were taken at constant exposure time at 40x magnification by employing Olympus BX-51 microscope coupled to DP-70 digital camera, and CellSens Dimension visualisation and quantification software (Olympus, Tokyo, Japan). The unprocessed green channel images were converted to grayscale, and the ventral horn cSNAP-25 immunoreactivity was quantified as an average pixel-thresholded area (pixel intensity 100-256) in 6 non-overlapping visual fields per each L4 coronal section (6 x 0.14 mm^2 total analysed area per slice). This was performed in 4 randomly chosen L4 coronal spinal cord slices per each animal as previously described (Matak 2020). The confocal imaging of stained spinal cord slices at level of ventral horn to evaluate colocalization was done with Olympus FV3000 microscope and a 60× oil-immersion objective (UplanSApo, NA1.35, Olympus, Tokyo, Japan) using FV10-ASW software with 5 X scan zoom at a resolution of 1024×1024 pixels. Signal bleed-through was minimised by adjusting the excitation line of laser, power intensity, and emission range chosen independently for each fluorophore and different samples. The Fiji software was used for raw picture processing without altering the intensity of the signal. The representative images shown in figures were processed for brightness and contrast in Adobe Photoshop (Adobe Systems, San Jose, CA, USA). Muscle slices on glass were washed by PBST and blocked in 10% NGS. Incubation with anti BoNT-A-cleaved SNAP-25 (1:4000, diluted in 1% NGS and PBST) was carried out overnight at room temperature, followed next day by 1:400-500 goat anti-rabbit Alexa 555 secondary antibody (Cell Signalling, Danvers, USA), and coverslipped with anti-fading agent. Semi-quantification of the cleaved SNAP-25 was performed as previously described (Šoštarić et al., 2022; Perier et al., 2021). Briefly, in muscle slices from each animal, 4 visual fields from 4 different slices were chosen and scored (0-4) based on presence and abundance of clSNAP-25 in NMJs, nerve terminals and axons (Supplementary file S1).

Table 1. The list of primary and secondary antibodies used in the immunofluorescent colocalization stainings, with dilutions and incubation conditions.

Primary antibody	dilution	incubation temperature and period	catalog no/company	host species
anti-ChAT monoclonal	1:2500	4 °C overnight	AMAB91130/Atlas Antibodies	mouse
anti-SV2C [a] clone 4C8.1 monoclonal	1:1000	4 °C overnight	MABN367/Milipore	mouse
anti-K_v2.1.[b] monoclonal	1:1000	4 °C overnight	ab192761/Abcam	mouse
anti-Synaptophysin monoclonal	1:1000	4 °C overnight	S5678/Sigma Aldrich	mouse
anti-Vglut1[c] polyclonal	1:5000	4 °C overnight	135304/Synaptic Systems	guinea pig
secondary antibody				
anti-rabbit polyHRP[d]	undiluted	room temperature, 1 h	B40923/Invitrogen (from Tyramide SuperBoost Kit)	goat
anti-mouse IgG Fab2 Alexa Fluor 555	1:400-1:500	room temperature, 2 h	4490S/CellSignaling Technology	goat
anti-guinea pig IgG H&L Alexa Fluor 555	1:400	room temperature, 2 h	ab150186 /abcam	goat

anti-rabbit IgG Fab2 Alexa Fluor 555	1:400	room temperature, 2 h	4413S/CellSignaling Technology	goat

[a]synaptic vesicle protein 2 C, [b] potassium voltage channel K_v2.1., [c] vesicular glutamate transporter 1, [d]horseradish peroxidase-polyconjugated

2.7. Statistical analysis

Results are presented as mean ± SEM and analysed by two-way ANOVA for repeated measurements, followed by Bonferroni's multiple post hoc test (P <0.05 considered significant) for between-group comparisons. The non-parametric ANOVA (Kruskal Vallis) and Dunn's post hoc were employed for statistical analysis of non-normally distributed Csnap-25 immunoreactive area (median ± range with P<0.05 considered significant). Single measurement of gastrocnemius and soleus muscle weight was analysed by one-way ANOVA followed by Bonferroni's multiple comparison test.

The number of animals per treatment group determination was performed according to *a priori* power analysis performed with G*power software version 3.1. (University of Düsseldorf, Germany) based on estimated effect size F=0.4, α error probability = 0.05, power (1-β) = 0.9, statistical test: ANOVA: repeated measures, within-between interaction (Šoštarić et al., 2022; Charan and Kantharia, 2013). In addition, we extended the group size from 6 to 8 to account for possible attrition of animals during the experiment.

3. Results

Presently, to assess the BoNT-A actions on central locomotor circuits, we characterised its trans-synaptic effect on normal motor performance involving coordinated use of hind limbs. An optimised method to study its central effects includes BoNT-A injection into the peripheral sciatic nerve trunk that, in contrast to i.m. injection, avoids the masking of the central toxin action (Matak 2020). The participation of central toxin effect through its action on second order central synapses was assessed by combining the BoNT-A treatment with

subsequent intrathecal lumbar injection of equine BoNT-A-neutralising antitoxin to prevent the central transcytosis, as previously reported (Matak 2020).

3.1. Lasting impairment of motor coordination and performance is mediated by transcytosis-dependent central action of BoNT-A

Firstly, we examined the effect of BoNT-A on fine motor coordination and balance by employing beam walking and rotarod tests. Prior to BoNT-A i.n. injection, the animals were pre-trained to traverse swiftly across the narrow beam and maintain balance on the rotating rod during the maximal trial duration. The animals injected i.n. with saline and i.t. with horse serum did not show signs of motor impairment after surgeries, suggesting the lack of effect due to control treatments and i.n. or i.t. injection procedures itself. Animals treated with i.n. BoNT-A (+ horse serum i.t.) approximately doubled the transit time across the narrow beam at day 3 after the toxin injection. The performance started to recover gradually after day 7, and returned to normal pretreatment values by day 28-35 (figure 2A). The BoNT-A also induced a prominent impairment of the animals' ability to maintain the balance on the rotarod (reduced latency to fall) which peaked between day 7-14 and thereafter started to recover gradually, yet never fully by day 56 (figure 2B). Prevention of spinal toxin transcytosis by intrathecal lumbar injection of BoNT-A-neutralizing antitoxin prevented the motor deficits evoked by i.n. BoNT-A in both of these motor performance tests. Animals injected with i.n. BoNT-A in combination with the i.t. antitoxin exhibited a very mild deficit in the rotarod performance by day 3, which subsequently recovered, and did not display any apparent deficit in the beam transit time at any experimental time point (figure 2).

To account for the possible effect of the BoNT-A on motor activity involving intense motoneuronal activation, we examined its effect on swimming performance. Swimming as a high-output motor task, is dependent on cholinergic modulation mediated by C-boutons, synapses responsible for alterations in motoneuron firing rate (Zagoraiou et al., 2009; Konsolaki et al., 2020). We found that i.n. BoNT-A significantly reduces mean (figure 2C) and maximal swimming velocities (figure 2D), which recovered by day 36 post toxin treatment.

Again, the toxin-mediated swimming velocity reduction was fully prevented by the i.t. antitoxin (figure 2C, figure 2D).

Figure 2.

In addition to motor performance tests, we examined the hind paw appearance suggestive of localised muscle weakness during reflex toe spread and gait. The rats showed mild impairment of the toe-spreading reflex (DAS ≈ 1) that quickly recovered by day 21 (figure 3A). The BoNT-A i.n. treatment reduced the functional use of hindlimbs and markedly changed the appearance of hind paws during stance. The hind paws exhibited arch-like appearance of foot soles and toes, and the heel-supported weight bearing, indicative of the weakness of paw plantar flexors (figure 3B) Moreover, the animals were unable to perform a normal foot propulsion during terminal stance by using interdigital paw pads and toes. This resulted in reduced combined gait ability score (sum of scores from five different parameters ranging from 0-10) used to evaluate voluntary motor function. The antitoxin-treated animals also exhibited a reduced gait ability following i.n. BoNT-A, however, with milder impairment and accelerated recovery of motor function (figure 3B).

Figure 3.

3.2. The BoNT-A induces muscle atrophy independent of its central action

We further assessed the i.n. BoNT-A effect on measurable signs of muscular atrophy by monitoring the calf diameter throughout the experiment and by measuring muscle weights at the end of experiment. We observed a significant reduction of the estimated mid-calf cross-section area of BoNT-A-treated hind limbs (figure 4A), as well as the final gastrocnemius muscle weight (figure 4B). Seemingly, the BoNT-A + antitoxin - treated animals showed slightly lower reduction of estimated cross section area (figure 4A), however, the reduction of the gastrocnemius muscle weight by i.n. BoNT-A was not dependent on the toxin central transcytosis (figure 4B). In contrast to gastrocnemius, there was no observable difference of the soleus muscle weight between the experimental groups (figure 4C). Changes in muscle

size were not accompanied by significant changes in animal body weight throughout the experiment, eliminating possible systemic effect of i.n. BoNT-A (figure 4D).

Figure 4.

3.3. Axonally transported and transcytosed BoNT-A reduces local spastic paralysis without altering the exaggerated monosynaptic H-reflex

After the recovery of major motor functions roughly two months after BoNT-A injection, we examined the persistence of its antispastic action by using TeNT-evoked disinhibition of motoneuronal inhibitory control. The BBB locomotor scale, which is used to evaluate locomotor recovery after different spinal cord injuries, was used to assess the functional use of limbs during locomotion on a flat surface. Animals' locomotion and lower limb movement was monitored and evaluated with scores (with 21 rating highest and validating normal locomotion, to 0 rating the lowest and describing no observable movement of the limb) (Basso et al., 1995). Starting from day 3 after TeNT, control animals treated with saline developed a prominent spastic paralysis of the injected right hindlimb, manifested as the leg rigid extension and inability to fully flex the joint. The locomotor impairment, evident as sweeping of affected hind limb against the table surface without weight support or plantar stepping during locomotion, resulted in markedly reduced BBB score. The i.n. BoNT-A reduced the dorsiflexion resistance from days 3-15 (figure 5C) and partly counteracted the locomotor impairment on day 15 post TeNT, showing improved use of plantar hind paw surface and weight bearing scoring higher on the BBB scale (figure 5A, figure 5D) The beneficial BoNT-A action was prevented in the i.t. antitoxin-treated rats, evident as high passive resistance during dorsiflexion test (figure 5C) and impaired locomotor score similar to saline-treated animals (figure 5B and figure 5D).

Figure 5.

In addition to behavioural assessment, we employed EMG to examine possible BoNT-A effects on monosynaptic H reflex transmitted by central synapse between Ia afferents and

motoneurons, evoked by subcutaneous electrical stimulation over the sciatic nerve. As previously shown (Matthews et al., 2014), the i.m. TeNT induced a large increase of H_{max} amplitude peaking on day 8 post injection in all experimental groups. Interestingly, the H-reflex excitability started to recover faster than the leg spasm intensity or locomotor deficit by day 15 post TeNT, suggesting that the sustenance of TeNT-evoked muscle spasm (figure 5) is not associated with persistence of overactive monosynaptic reflex. We found that i.n. BoNT-A reduced the maximal amplitude of M-wave and H-reflex prior to, and on day 8 post TeNT with no apparent difference with the antitoxin treatment (figure 6A, figure 6B). However, when the H-reflex amplitude was corrected for the size of M_{max} and the muscle weight, the effect of the BoNT-A was not significantly different compared to controls (figure 6C, figure 6D), indicating the lack of BoNT-A effects on monosynaptic reflex excitability. In accordance, we observed lack of colocalization of BoNT-A-cleaved SNAP-25 with VGlut1 isoform of the glutamate transporter figure 6E), suggesting the lack of direct toxin effect on the central afferent terminal of Ia primary afferents involved in the monosynaptic stretch reflex.

Figure 6.

3.4. The i.n. BoNT-A cleaves SNAP-25 in peripheral motor terminals and central second order synapses

At the end of the experiment (day 78) we examined the sites of BoNT-A enzymatic action by immunodetection of its enzymatic products in the periphery and CNS. In the gastrocnemius muscles of animals treated with BoNT-A we found cleaved SNAP-25 in neuromuscular junctions, nerve terminals and axons. Their relative abundance was not affected by the antitoxin treatment (figure 7A, figure 7C). On the other hand, the amount of cSNAP-25 in the ventral horn was reduced by the i.t. antitoxin (figure 7B, figure 7D), indicating central toxin transcytosis.

Figure 7.

In addition to VGlut1, we analysed the colocalization of the toxin enzymatic activity in relation to other synaptic markers and known toxin acceptors. We found that a portion of BoNT-A-cleaved SNAP-25 was present in ChAT-expressing neurons and contacted the K_v2.1. immunoreactivity, suggesting that at least the fraction of toxin's central effect is associated with the C-boutons (figure 8A, figure 8B). In contrast to partial colocalization with ChAT, the majority of cleaved-SNAP-25-containing terminals colocalized with the BoNT-A nerve terminal protein acceptor SV2C and synaptic marker synaptophysin (figure 8C, figure 8D). Apparently, both SV2C and synaptophysin were present in higher number of cSNAP-25-immunopositive terminals in comparison to the ChAT and K_v2.1., suggesting that different types of nerve terminals, including both cholinergic and non-cholinergic, are susceptible to BoNT-A enzymatic activity following its axonal transport and transcytosis.

Figure 8.

4. Discussion

Intramuscular BoNT-A is a standard treatment for different movement disorders characterised by sustained or intermittent muscle hyperactivity. The currently dominant opinion is that BoNT-A actions in hyperkinetic/hypertonic muscle result from direct toxin's action on extrafusal plus either direct or indirect modulation of intrafusal muscle terminals, followed by indirect plastic changes in the CNS (Rosales and Dressler, 2010; Hallet 2018). In the rat motor system, as previously mentioned, we found that the toxin transcytosis at spinal cord level participates in the lasting reduction of TeNT-evoked local spasm (Matak 2020; Šoštarić et al., 2022). Though its peripheral action is well described at the level of extrafusal neuromuscular junction, a general picture of all the possible sites of BoNT-A actions at multiple levels of motor processing is still lacking. In addition, it remains so far unknown if the central toxin action affects different spinal synapses as vital elements of circuits involved in normal locomotion.

To address this later question, we studied the behavioural actions of BoNT-A on motor tasks involving multiple muscle groups on both hindlimbs. The BoNT-A was injected bilaterally

into the sciatic nerve trunk at mid-thigh level to affect all the motor units of the lower leg and foot (indirectly innervated by sciatic nerve via common peroneal and tibial nerve) by anterograde and retrograde axonal transport (Antonucci et al., 2008; Restani et al., 2011). We then examined the effect of BoNT-A on fine motor coordination and balance in skilled motor performance tasks involving simultaneous bilateral use of multiple muscle groups with quick alternations of contractions of flexors and extensors. The BoNT-A bilateral injection into the sciatic nerves markedly reduced the motor performance in both tasks (figure 2A, figure 2B), with faster recovery of the beam walk performance by day 28 in comparison to rotarod performance incomplete recovery (examined up to day 56). In contrast to bilateral i.n. BoNT-A, unilateral i.n. BoNT-A induces only mild impairment in the beamwalk performance, and no observable impairment in the rotarod latency (Matak 2020), suggesting the compensation of motor deficits by the untreated contralateral limb in mentioned motor tasks. In addition to neuromuscular coordination we monitored the development of classical signs of local muscle weakness by assessing the reflex digit abduction and paw appearance during gait. The animals developed very mild toe-spreading reflex deficit (DAS ≈ 1 out of maximal 4 normally observed for the same toxin dose injected i.m.) that quickly recovered within 14 days after BoNT-A treatment (figure 3A). Other signs of muscle weakness such as the arched position of hind paws during motor activities like sitting, bipedal stance or climbing measured by combined „gait ability“ score (Brent et al., 2020; Warner et al., 2006) suggested lasting weakness of plantar flexors that support the body weight and mediate the limb propulsion during the terminal stance (figure 3B). Mentioned impairment took longer to recover compared to DAS with recovery time-course comparable to rotarod.

We assessed the role of central transcytosis-dependent toxin activity by employing the BoNT-A-specific antitoxin injection into the spinal canal at the level of cauda equina 24 h after i.n. toxin injection. In all the aforementioned motor tests or functional outcomes, the BoNT-A-evoked motor deficits were either prevented or reduced in intensity and duration in rats injected with i.t. antitoxin (figure 2, figure 3). This suggests that BoNT-A trans-synaptic

activity in second order spinal synapses, in concert with peripheral toxin action, affects motor performance in different tests and contributes to local muscle weakness. Consistent with the dual site of toxin action, we found that cSNAP-25 occurred both peripherally and centrally, with only the central enzymatic activity being dependent on the toxin transcytosis (figure 7). On the other hand, calf muscle weight and CMAP reduction occurred at similar intensity in all toxin-treated animals, suggesting a peripheral toxin action as the main driver of muscle atrophy and residual effect on NMJ transmission (figure 4B, figure 6A). In contrast to gastrocnemius, the dominantly slow-twitch fibre soleus muscle did not show atrophy, indicating possible faster recovery of this type of muscle (figure 4C).

After assessment of locomotor recovery, in the same animals we additionally examined if BoNT-A may induce central modulation of exaggerated monosynaptic stretch reflex that is clinically observed in spasticity (Rosales and Dressler, 2010; Stampacchia et al., 2004), with TeNT-evoked unilateral spasm used as a convenient model of neuromuscular spasticity of central origin (Megighian et al., 2021). We observed that BoNT-A retained the ability to reduce the TeNT-evoked calf spasm on days 65-77 despite all peripheral motor parameters being substantially or completely recovered by day 56. This effect was, again, found to be dependent on BoNT-A central trans-synaptic effect (figure 5). In contrast to BoNT-A-mediated reduction of spasm and locomotor deficit, the effect of BoNT-A on the monosynaptic reflex excitability (assessed by H_{max} / M_{max} ratio) was not significant, both prior to and after TeNT-evoked spasticity (figure 6C) and in line with a lack of cleaved SNAP-25 colocalization with large synaptic terminals positive for VGlut1, the marker of Ia terminals (Rotterman et al., 2014) (figure 6E). This suggests lack of BoNT-A central activity on the synaptic strength between Ia central afferent terminals and motoneurons, in line with previous clinical studies reporting the lack of BoNT-A on the H/M ratio (Priori et al., 1995; Modugno et al., 1998; Phadke et al., 2013; Manca et al., 2010). However, H-reflex induction by peripheral nerve electrical stimulation bypasses the normal stretch reflex initiation at muscle spindles, thus, not assessing possible BoNT-A direct or indirect actions at peripheral intrafusal terminals. Nevertheless, our findings

show that normalisation of experimental spasm involves central trans-synaptic action of the toxin, thus, indicating a more complex mechanism of BoNT-A action other than stretch reflex direct modulation.

To further address the possible sites of BoNT-A action in the CNS we performed colocalization of cleaved SNAP-25 with additional neuronal markers. It was observed that BoNT-A may enzymatically cleave the SNAP-25 in ChAT- and VAChT-expressing cholinergic terminals (Matak et al., 2012; Caleo et al., 2018; Cai et al., 2017), with comparably higher selectivity for cholinergic synapses compared to other types (Caleo et al., 2018), suggesting its possible trans-synaptic effect on C-boutons synapsing with motoneuronal cell bodies. This premotor input derived from $V0_C$ interneurons supports the motoneuronal firing in demanding motor tasks such as swimming (Zagoraiou et al., 2009). In accordance, we found that BoNT-A impairs the swimming velocity (Figure 3), and that a fraction of cSNAP-25-containing terminals expressed ChAT or contacted the $K_v2.1$-expressing postsynaptic sites typically associated with C-boutons (figure 8A, figure 8B). Yet, the occurrence of cSNAP-25 in comparably more numerous SV2C- and synaptophysin-expressing terminals (figure 8C, figure 8D) suggests toxin transcytosis to additional non-cholinergic central synapses that possess the main protein acceptor for BoNT-A (Verderio et al., 2007) and the synaptic neurotransmitter release machinery (Figure 9). The BoNT-A action within different premotor neurons is also in line with behavioural effect on other examined motor functions besides swimming. Interestingly, genetic ablation of cholinergic C boutons does not affect the rotarod performance in mice (Konsolaki et al., 2020), suggesting that BoNT-A action in C-boutons cannot explain the reduction of rotarod performance observed here. In support of its action in other central excitatory synapses, BoNT-A preferentially inhibits the release of glutamate in comparison to GABA in isolated hippocampal synaptosomes (Mahrhold et al., 2006). Apart from neurotransmitter release, BoNT-A may alter other SNAP-25-mediated functions in synaptic and extrasynaptic sites, e.g. Ca^{2+} dynamics mediated by SNAP-25 interactions with synaptotagmin, presynaptic voltage-gated Ca^{2+}channels and G proteins (Pozzi et al., 2019) ,

as well as the translocation of membrane proteins and channels (Shimizu et al., 2012). These complex actions might be associated with net balance in favour of reduction of premotor neuronal network activity. These effects are likely to contribute to desirable restoration of muscle control in disinhibited motor circuits in movement disorders or spasticity (Liu et al., 2015; Bellardita et al., 2017; Pocratsky et al., 2023).

Figure 9.

Some of the cleaved SNAP-25 may be present in recurrent axonal collaterals due to BoNT-A axonal transport without trans-synaptic transport, since the toxin would not necessarily need to exit and re-enter the motoneuron from extracellular fluid (and be neutralized by antitoxin). Our experiments do not exclude this option, however, given the specific role of recurrent collaterals only partially contributing to activation of Renshaw cells in recurrent and reciprocal inhibition, the central BoNT/A behavioral actions on many locomotor functions and TeNT-evoked spasm (evoked by TeNT affecting different types of inhibitory interneurons along Renshaw cells), preventable by antitoxin, likely cannot be explained exclusively by such action.

In spastic or dystonic limb/regions, targeting different muscles is assumed to be the only feasible mode of BoNT-A injection. Herein we show that toxin injection into the peripheral nerve enables simultaneous targeting of different muscles at peripheral and spinal synaptic sites relevant for their neuromotor control. The characterization of antero-retrograde effects of the toxin substantiates that the effect is similar to i.m. injection, with the advantage that the i.n. injection mode avoids the initial full paralysis due to BoNT-A entry at the NMJ. Nonetheless, it attenuates muscle hyperactivity for a long time. This better approximates the clinical observations that BoNT-A-mediated benefit is not necessarily accompanied by prominent muscle paralysis (Hallet 2018). The i.n. mode of toxin delivery might complement the muscular toxin injections employed clinically. Toxin application by existing nerve block techniques that avoid the nerve injury (Jeng and Rosenblatt , 2011) might provide an alternative way to target regional muscle groups innervated by the common nerve/nerve branches. In addition, it may

complement already existing nerve block techniques with general anaesthetics or neurolytic agents aimed at spasticity management (Picelli et al., 2023). Interestingly, case studies reported successful BoNT-A intra- or peri-nerve application in chronic pain patients (Ryu et al., 2019; Mercado et al., 2023). The studies showed no apparent signs of nerve injury occurring after BoNT-A i.n. injections (Matak 2020; Bach-Rojecky and Lacković, 2009; Mercado et al., 2023; Lu et al., 1998).

In comparison to human subjects, it is important to note that a limiting factor in this study is that the research was exclusively conducted on male rats to achieve more uniform weight and dosing. In addition, the crude measurements of muscle weight and cross-section area as a measure of atrophy performed here cannot distinguish, specifically, the possibility that the restoration of muscle mass, normal movement and force may be attributed to hypertrophy in some fibers, while others may not exhibit similar improvements.

5. Conclusion

Up to now, BoNT-A local muscular neuroparalytic effects have been regarded as its only physiological correlate of therapeutically desirable effect in spasticity and movement disorders [26]. Present study shows that its actions affect the gait and motor functions on both peripheral and central level. Further, our behavioural and colocalization studies suggest that BoNT-A activity in the ventral horn does not necessarily restrict to a single-type synapse, but rather to interplay between different central circuits involved in normal locomotion and involuntary hyperactive movement.

ACKNOWLEDGEMENTS

This research was funded by the Croatian Research Foundation (project no. HRZZ UIP-2019-04-8277). Lyophilized polyclonal equine IgG-based BoNT-A antitoxin (NIBSC code 14/174) and non-affinity purified rabbit polyclonal antibody to BoNT-A-cleaved SNAP-25 recognizing the SNAP-25 1–197 fragment were a kind gift from Dr. Thea Sesardic (National Institute for Biological Standards and Control, Potters Bar, United Kingdom). The funding source had no

role in study design; collection, analysis and interpretation of data, writing and decision to submit the article.

AUTHOR CONTRIBUTIONS

IM: Conception and design of the study; PŠ, MM, DV, ŽLV, MP, MC, IM: Acquisition and analysis of the data; PŠ, IM: Draft of the manuscript and figures; All authors revised and approved the final manuscript.

ADDITIONAL INFORMATION

Conflict of interests: The authors declare no conflict of interests.

REFERENCES

Anandan C, Jankovic J. Botulinum toxin in movement disorders: An update. Toxins. 2021;13:42. doi: 10.3390/toxins13010042.

Antonucci F, Rossi C, Gianfranceschi L, Rossetto O, Caleo M. Long-distance retrograde effects of botulinum neurotoxin A. J Neurosci. 2008; 28: 3689–96. doi: 10.1523/JNEUROSCI.0375-08.2008

Aymard C, Giboin LS, Lackmy-Vallée A, Marchand-Pauvert V. Spinal plasticity in stroke patients after botulinum neurotoxin A injection in ankle plantar flexors. Physiol Rep. 2013; 1:e00173. doi: 10.1002/phy2.173.

Bach-Rojecky L, Lacković Z. Central origin of the antinociceptive action of botulinum toxin type A. Pharmacol Biochem Behav. 2009; 94:234–8. doi:10.1016/j.pbb.2009.08.012.

Basso DM, Beattie MS, Bresnahan JC. A sensitive and reliable locomotor rating scale for open field testing in rats. J Neurotrauma. 1995; 12:1–21. doi:10.1089/neu.1995.12.1.

Bellardita C, Caggiano V, Leiras R, Caldeira V, Fuchs A, Bouvier J, Löw P, Kiehn O. Spatiotemporal correlation of spinal network dynamics underlying spasms in chronic spinalized mice. Elife. 2017;6:e23011. doi: 10.7554/eLife.23011.

Brent MB, Lodberg A, Thomsen JS, Brüel A. Rodent model of disuse-induced bone loss by hind limb injection with botulinum toxin A. MethodsX. 2020; 7:101079. doi: 10.1016/j.mex.2020.101079.

Broide R, Rubino J, GS Nicholson, Ardila M, Brown M, Aoki K, et al. The rat Digit Abduction Score (DAS) assay: a physiological model for assessing botulinum

neurotoxin-induced skeletal muscle paralysis. Toxicon. 2013; 71:18–24. doi: 10.1016/j.toxicon.2013.05.004.

Brooks VB, Curtis DR, Eccles JC. The action of tetanus toxin on the inhibition of motoneurones. J Physiol. 1957; 135:655–72. doi: 10.1113/jphysiol.1957.sp005737.

Cai BB, Francis J, Brin MF, Broide RS. Botulinum neurotoxin type A-cleaved SNAP25 is confined to primary motor neurons and localized on the plasma membrane following intramuscular toxin injection. Neuroscience. 2017; 352:155–69. doi: 10.1016/j.neuroscience.2017.03.049.

Caleo M, Mazzocchio R. Direct Central Nervous System Effects of Botulinum Neurotoxin. From Dressler D; Altenmüller E, Krauss Joachim K. (2018). Treatment of Dystonia. Publisher: Cambridge University Press, pp. 111–114. doi:10.1017/9781316459324.025

Caleo M, Spinelli M, Colosimo F, Matak I, Rossetto O, Lackovic Z, et al. Transynaptic action of botulinum neurotoxin type A at central cholinergic boutons. J Neurosci. 2018; 38:10329–37. doi: 10.1523/JNEUROSCI.0294-18.2018.

Carter RJ, Morton J, Dunnett SB. Motor coordination and balance in rodents. Curr Protoc Neurosci. 2001;Chapter 8. doi: 10.1002/0471142301.ns0812s15. doi: 10.1002/0471142301.ns0812s15.

Charan J, Kantharia ND. How to calculate sample size in animal studies? J Pharmacol Pharmacother. 2013; 4:303–6. doi: 10.4103/0976-500X.119726.

Ekong TAN, Feavers IM, Sesardic D. Recombinant SNAP-25 is an effective substrate for Clostridium botulinum type A toxin endopeptidase activity in vitro. Microbiol. 1997; 143:3337–47. doi: 10.1006/exnr.2002.8013.

Gracies JM. Physiological effects of botulinum toxin in spasticity. Mov Disord. 2004;19 Suppl 8:120-128. doi: 10.1002/mds.20065.

Gundersen CB. The effects of botulinum toxin on the synthesis, storage and release of acetylcholine. Prog Neurobiol. 1980; 14 (2-3):99-119. doi:10.1016/0301-0082(80)90019-2.

Hallett M. Mechanism of action of botulinum neurotoxin: Unexpected consequences. Toxicon. 2018;147:73–6. doi: 10.1016/j.toxicon.2017.08.011.

Ho SM, Waite PM. Effects of different anesthetics on the paired-pulse depression of the H reflex in adult rat. Exp Neurol. 2002; 177:494–502.

Homolak J, Babic Perhoc A, Knezovic A, Osmanovic Barilar J, Koc F, Stanton C, et al. Disbalance of the duodenal epithelial cell turnover and apoptosis accompanies insensitivity of intestinal redox homeostasis to inhibition of the brain glucose-dependent insulinotropic polypeptide receptors in a rat model of sporadic Alzheimer's disease. Neuroendocrinology. 2022; 112:744–62. doi: 10.1159/000519988.

Jankovic J. Botulinum toxin: State of the art. Mov Disord. 2017;32:1131–8. doi: 10.1002/mds.27072.

Jeng CL, Rosenblatt MA. Considerations When performing ultrasound-guided supraclavicular perineural catheter placement. J Ultrasound Med. 2011; 30:423–423. doi: 10.7863/jum.2011.30.3.423.

Jones RGA, Ochiai M, Liu Y, Ekong T, Sesardic D. Development of improved SNAP25 endopeptidase immuno-assays for botulinum type A and E toxins. J Immunol Methods. 2008; 329:92–101. doi: 10.1016/j.jim.2007.09.014.

Koizumi H, Goto S, Okita S, Morigaki R, Akaike N, Torii Y, et al. Spinal central effects of peripherally applied botulinum neurotoxin A in comparison between its subtypes A1 and A2. Front Neurol. 2014; 5:1–9. doi: 10.3389/fneur.2014.00098.

Konsolaki E, Koropouli E, Tsape E, Pothakos K, Zagoraiou L. Genetic inactivation of cholinergic C bouton output improves motor performance but not survival in a mouse

model of amyotrophic lateral sclerosis. Neuroscience. 2020 ; 450:71–80. doi: 10.1016/j.neuroscience.2020.07.047.

Laliberte AM, Goltash S, Lalonde NR, Bui TV. Propriospinal Neurons: Essential Elements of Locomotor Control in the Intact and Possibly the Injured Spinal Cord. Front Cell Neurosci. 2019 Nov 12;13:512. doi: 10.3389/fncel.2019.00512.

Li D, Mattoo P, Keller JE. New equine antitoxins to botulinum neurotoxins serotypes A and B. Biologicals. 2012; 40:240–6. doi: 10.1016/j.biologicals.2012.03.004.

Liu YB, Tewari A, Salameh J, Arystarkhova E, Hampton TG, Brashear A, Ozelius LJ, Khodakhah K, Sweadner KJ. A dystonia-like movement disorder with brain and spinal neuronal defects is caused by mutation of the mouse laminin β1 subunit, Lamb1. Elife. 2015 Dec 24;4:e11102.

Lu L, Atchabahian A, Mackinnon SE, Hunter DA. Nerve injection injury with botulinum toxin. Plast Reconstr Surg. 1998; 101:1875–80. doi:10.1097/00006534-199806000-00015.

Mahrhold S, Rummel A, Bigalke H, Davletov B, Binz T. The synaptic vesicle protein 2C mediates the uptake of botulinum neurotoxin A into phrenic nerves. FEBS Lett. 2006; 580:2011–4. doi: 10.1016/j.febslet.2006.02.074.

Manca M, Merlo A, Ferraresi G, Cavazza S, Marchi P. Botulinum toxin type A versus phenol. A clinical and neurophysiological study in the treatment of ankle clonus. Eur J Phys Rehabil Med. 2010; 46:11–8. PMID: 20332721

Marchand-Pauvert V, Aymard C, Giboin LS, Dominici F, Rossi A, Mazzocchio R. Beyond muscular effects: depression of spinal recurrent inhibition after botulinum neurotoxin A. J Physiol. 2013; 591:1017–29. doi: 10.1113/jphysiol.2012.239178.

Matak I, Lacković Z, Relja M. Botulinum toxin type A in motor nervous system: unexplained observations and new challenges. J Neural Transm (Vienna). 2016;123:1415-21, doi: 10.1007/s00702-016-1611-9.

Matak I, Lacković Z. Botulinum toxin A, brain and pain. Prog Neurobiol. 2014 Aug-Sep;119-120:39-59. doi: 10.1016/j.pneurobio.2014.06.001. PMID: 24915026.

Matak I, Riederer P, Lacković Z. Botulinum toxin's axonal transport from periphery to the spinal cord. Neurochem Int. 2012; 61:236–9. doi: 10.1016/j.neuint.2012.05.001

Matak I. Evidence for central antispastic effect of botulinum toxin type A. Br J Pharmacol. 2020; 177:65–76. doi: 10.1111/bph.14846.

Matthews CC, Fishman PS, Wittenberg GF, Matthews CC. Tetanus toxin reduces local and descending regulation of the H-reflex. Muscle Nerve. 2014; 49:495–501. doi: 10.1002/mus.23938.

Mazzocchio R, Caleo M. More than at the neuromuscular synapse: actions of botulinum neurotoxin A in the central nervous system. Neuroscientist. 2015 Feb;21(1):44-61. doi: 10.1177/1073858414524633. PMID: 24576870.

Megighian A, Pirazzini M, Fabris F, Rossetto O, Montecucco C. Tetanus and tetanus neurotoxin: From peripheral uptake to central nervous tissue targets. J Neurochem. 2021; 158:1244–53. doi: 10.1111/jnc.15330.

Mercado M del PA, Olea MS, Rodrigues AT, Morales KE, Ros JJL, Altinpulluk EY, et al. Intraneural injection of botulinum toxin-A in palliative care and unresponsive neuropathic pain. Asia Pac J Pain. 2023. In press:1–6. doi: 10.29760/APJP.202302/PP.0001

Modugno N, Priori A, Berardelli A, Vacca L, Mercuri B, Manfredi M. Botulinum toxin restores presynaptic inhibition of group Ia afferents in patients with essential tremor. Muscle Nerve. 1998; 21:1701–5. doi: 10.1093/brain/118.3.801.

Percie du Sert N, Hurst V, Ahluwalia A, Alam S, Avey MT, Baker M, et al. The ARRIVE guidelines 2.0: Updated guidelines for reporting animal research. PLoS Biol. 2020;18:e3000410. doi: 10.1371/journal.pbio.3000410.

Périer C, Martin V, Cornet S, Favre-Guilmard C, Rocher MN, Bindler J, et al. Recombinant botulinum neurotoxin serotype A1 in vivo characterization. Pharmacol Res Perspect. 2021; 9:e00857. doi: 10.1002/prp2.857.

Phadke CP, On AY, Kirazli Y, Ismail F, Boulias C. Intrafusal effects of botulinum toxin injections for spasticity: revisiting a previous paper. Neurosci Lett. 2013; 541:20–3. doi: 10.1016/j.neulet.2013.02.025.

Picelli A, Di Censo R, Zadra A, Faccioli S, Smania N, Filippetti M. Management of spastic equinovarus foot in children with cerebral palsy: An evaluation of anatomical landmarks for selective nerve blocks of the tibial nerve motor branches. J Rehabil Med. 2023; 55:jrm00370. doi: 10.2340/jrm.v55.4538.

Pirazzini M, Rossetto O, Eleopra R, Montecucco C. Botulinum neurotoxins: Biology, pharmacology, and toxicology. Pharmacol Rev. 2017; 69:200–35. doi:10.1124/pr.116.012658

Pocratsky AM, Nascimento F, Özyurt MG, White IJ, Sullivan R, O'Callaghan BJ, Smith CC, Surana S, Beato M, Brownstone RM. Pathophysiology of Dyt1-Tor1a dystonia in mice is mediated by spinal neural circuit dysfunction. Sci Transl Med. 2023; 15(694):eadg3904. doi: 10.1126/scitranslmed.adg3904.

Pozzi D, Corradini I, Matteoli M. The control of neuronal calcium homeostasis by SNAP-25 and its impact on neurotransmitter release. Neuroscience. 2019; 420:72–8. doi: 10.1016/j.neuroscience.2018.11.009.

Priori A, Berardelli A, Mercuri B, Manfredi M, Neurologiche S, La R, et al. Physiological effects produced by botulinum toxin treatment of upper limb dystonia. Changes in reciprocal inhibition between forearm muscles. Brain. 1995; 118:801–7. doi: 10.1093/brain/118.3.801.

Ramachandran R, Yaksh TL. Therapeutic use of botulinum toxin in migraine: mechanisms of action. Br J Pharmacol. 2014 Sep;171(18):4177-92. doi: 10.1111/bph.12763. PMID: 24819339; PMCID: PMC4241086.

Ramirez-Castaneda J, Jankovic J, Comella C, Dashtipour K, Fernandez HH, Mari Z. Diffusion, spread, and migration of botulinum toxin. Mov Disord. 2013 Nov;28(13):1775-83. doi: 10.1002/mds.25582. Epub 2013 Jul 18. PMID: 23868503.

Restani L, Antonucci F, Gianfranceschi L, Rossi C, Rossetto O, Caleo M. Evidence for anterograde transport and transcytosis of botulinum neurotoxin A (BoNT/A). J Neurosci. 2011; 31:15650–9. doi: 10.1523/JNEUROSCI.2618-11.2011.

Restani L, Novelli E, Bottari D, Leone P, Barone I, Galli-Resta L, et al. Botulinum neurotoxin A impairs neurotransmission following retrograde transynaptic transport. Traffic. 2012; 13:1083–9. doi: 10.1111/j.1600-0854.2012.01369.x.

Rosales RL, Dressler D. On muscle spindles, dystonia and botulinum toxin. Eur J Neurol. 2010;17 Suppl 1:71-80. doi: 10.1111/j.1468-1331.2010.03056.x. PMID: 20590812.

Rossetto O, Montecucco C. Tables of toxicity of botulinum and tetanus neurotoxins. Toxins. 2019; 11:686. doi: 10.3390/toxins11120686.

Rossetto O, Pirazzini M, Montecucco C. Botulinum neurotoxins: Genetic, structural and mechanistic insights. Nat Rev Microbiol. 2014;12:535–49. doi: 10.1038/nrmicro3295.

Rotterman TM, Nardelli P, Cope TC, Alvarez FJ. Normal distribution of VGLUT1 synapses on spinal motoneuron dendrites and their reorganization after nerve injury. J Neurosci. 2014;34:3475–92. doi: 10.1523/JNEUROSCI.4768-13.2014.

Ryu JH, Shim JH, Yeom JH, Shin WJ, Cho SY, Jeon WJ. Ultrasound-guided greater occipital nerve block with botulinum toxin for patients with chronic headache in the

occipital area: a randomized controlled trial. Korean J Anesthesiol. 2019; 72:479–85. doi: 10.4097/kja.19145.

Schiavo G, Santucci A, Dasgupta BR, Mehta PP, Jontes J, Benfenati F, et al. Botulinum neurotoxins serotypes A and E cleave SNAP-25 at distinct COOH-terminal peptide bonds. FEBS Lett. 1993; 335:99–103. doi: 10.1016/0014-5793(93)80448-4.

Shimizu T, Shibata M, Toriumi H, Iwashita T, Funakubo M, Sato H, et al. Reduction of TRPV1 expression in the trigeminal system by botulinum neurotoxin type-A. Neurobiol Dis. 2012; 48:367–78. doi: 10.1016/j.nbd.2012.07.010.

Stampacchia G, Bradaschia E, Rossi B. Change of stretch reflex threshold in spasticity: effect of botulinum toxin injections. Arch Ital Biol. 2004; 142:265–73. Doi: 10.4449/aib.v142i3.375

Šoštarić P, Vukić B, Tomašić L, Matak I. Lasting peripheral and central effects of botulinum toxin type A on experimental muscle hypertonia in rats. Int J Mol Sci. 2022; 23:11626. doi: 10.3390/ijms231911626.

Verderio C, Grumelli C, Raiteri L, Coco S, Paluzzi S, Caccin P, et al. Traffic of botulinum toxins A and E in excitatory and inhibitory neurons. Traffic. 2007; 8:142-53. doi: 10.1111/j.1600-0854.2006.00520.x.

Vinti M, Costantino F, Bayle N, Simpson DM, Weisz DJ, Gracies JM. Spastic cocontraction in hemiparesis: Effects of botulinum toxin. Muscle Nerve. 2012;46:917–25. doi: 10.1002/mus.23427.

Warner SE, Sanford DA, Becker BA, Bain SD, Srinivasan S, Gross TS. Botox induced muscle paralysis rapidly degrades bone. Bone. 2006; 38:257–64. doi:10.1016/j.bone.2005.08.009.

Weise D, Weise CM, Naumann M. Central effects of botulinum neurotoxin—evidence from human studies. Toxins. 2019 Jan 1;11:21 doi: 10.3390/toxins11010021.

Zagoraiou L, Akay T, Martin JF, Brownstone RM, Jessell TM, Miles GB. A cluster of cholinergic premotor interneurons modulates mouse locomotor activity. Neuron. 2009; 64:645–62. doi: 10.1016/j.neuron.2009.10.017.

FIGURE LEGENDS

Figure 1. The time course and schematic representation of experimental treatments with bilateral intraneural (i.n.) botulinum toxin type A (BoNT-A), i.t. BoNT-A-neutralising antitoxin and unilateral i.m. tetanus toxin (TeNT), and functional behavioural motor testing in rats. The numbers above the timeline indicate experimental days following the i.n. BoNT-A treatment. H-reflex; Hoffmann's monosynaptic reflex; BBB, Basso Beattie Bresnahan locomotor scale. The figure was created with Biorender.com (*accessed on 22/09/2023*).

Figure 2. Botulinum toxin type A (BoNT-A) reduces the performance in motor coordination assays and swimming velocity dependently on its central trans-synaptic action. Spinal i.t. injection of BoNT-A-neutralizing antitoxin (5 iu) prevents the bilateral intraneural (i.n.) BoNT-A (2 U per sciatic nerve)-mediated impairment in beam walking A.) and rotarod B.) performances (evaluated by latency times) and reduces C.) mean swimming velocity and D.) maximal swimming velocity. N = 8 animals/ group; mean ± SEM, *,**,*** - P < 0.05, 0.01, 0.001 vs saline + horse serum; +, ++, +++ - P < 0.05, 0.01, 0.001 vs BoNT-A + horse serum (two-way RM ANOVA followed by Bonferoni's post hoc).

Figure 3. Intrasciatic BoNT-A induces mild temporary digit abduction inability and long-term prominent gait impairment, dependently on its central trans-synaptic action. The effect of bilateral intraneural (i.n.) BoNT-A (2 U per sciatic nerve) was assessed in combination with BoNT-A-neutralising antitoxin (5 iu, i.t.) on toe spreading reflex (assessed by digit abduction score) (A. and B.) and gait ability (C. and D.). The appearance of hind paws from BoNT-A-treated rats show the inability to abduct all toes A.) and the arch-like hind paw appearance C.) with heel-supported weight bearing during bipedal stance (left vs right: saline + horse serum vs BoNT-A + horse serum). In graph B.), horizontal lines indicate the time points of BoNT-A and antitoxin treatments. N = 8 animals/ group; mean ± SEM, *,**,*** - P < 0.05, 0.01, 0.001 vs saline + horse serum; +, ++, +++ - P < 0.05, 0.01, 0.001 vs BoNT-A + horse serum (two-way RM ANOVA followed by Bonferroni’s post hoc).

Figure 4. The i.n. BoNT-A induces non-recovering lower leg calf muscle atrophy. The graphs indicate A.) estimated lower leg cross section area during the experiment, and muscle weights of B.) gastrocnemius and C.) soleus on day 78 following i.n. BoNT-A (2 U per nerve) in combination with BoNT-A-specific antitoxin (5 iu). The effects of BoNT-A were unrelated to changes in total animal weight during the experiment D.). The leg cross section area was estimated as an ellipse area defined by dorsoventral and mediolateral diameter of the calf muscle (average of both legs). *N* = 8 animals/ group; mean ± SEM, *,**,*** - *P* < 0.05, 0.01, 0.001 vs saline + horse serum; + - *P* < 0.05 vs BoNT-A + horse serum (two-way RM ANOVA followed by Bonferroni's post hoc).

Figure 5. Lasting central antispastic activity of axonally transported BoNT-A. The intraneural (i.n.) BoNT-A (2 U per sciatic nerve) was administered in combination with BoNT-A-neutralising antitoxin (5 iu, i.t., 24 h post BoNT-A), and the spastic paralysis was evoked by i.m. tetanus toxin (TeNT) 1.5 ng injection into right gastrocnemius) on day 62 post BoNT-A. The photographs show the normal vs spastic hind-limb appearance of BoNT-A + horse serum A.) and BoNT-A + antitoxin-treated B.) animals on day 15 post TeNT. The spastic paralysis evoked by TeNT was quantified behaviourally by C.) resistance to ankle dorsiflexion and D.) Basso Beattie Bresnahan (BBB) locomotor scale. The vertical lines indicate the timepoint of TeNT treatment. *N* = 8 animals/ group; mean ± SEM,*** - *P* < 0.0015 vs saline + horse serum; ++,+++ - *P* < 0.01, 0.0015 vs BoNT-A + horse serum (two-way RM ANOVA followed by Bonferroni's post hoc).

Figure 6. Lack of BoNT-A action on the monosynaptic reflex excitability at the Ia central afferent synapse. The BoNT-A was injected into the sciatic nerve (2 U per nerve) in combination with intrathecal BoNT-A-neutralizing antitoxin. Electromyographic measurement of gastrocnemius CMAP was performed prior to tetanus toxin (TeNT, 1.5 ng i.m.), and after the development of TeNT-evoked local spasm by employing increasing voltage rectangular pulses (200 μs) delivered subcutaneously into the thigh over the sciatic nerve. The graphs A.)

and B.) show the effects of neurotoxins on peak to peak maximal M-wawe (M_{max}) and Hoffman or H-reflex (H_{max}) amplitudes, while C.) and D.) show the relation of H_{max} amplitude relative to M_{max}, and in relation to gastrocnemius muscle weight of individual rats, respectively. Each compound potential measurement is average of 3 maximal peak to peak amplitudes obtained during the measurement. *N* = 8 animals/ group; mean ± SEM, *,** - *P*< 0.05, 0.01 vs saline + horse serum (two-way RM ANOVA followed by Bonferroni's post hoc). In the L4 ventral horn of animals injected with i.n. BoNT-A, the BoNT-A-cleaved SNAP-25 (cSNAP-25) does not colocalize with vesicular glutamate transporter 1 (VGlut1) – the transporter isoform present in Ia muscle spindle primary afferents E.). The confocal microscope image represents a single optical slice (0.42 µm thickness) from confocal z-stack, representative from at least 3 different animals injected with i.n. BoNT-A + horse serum (scale bar = 20 µm).

Figure 7. Peripheral and central enzymatic activity of axonally transported BoNT-A. The intraneural (i.n.) BoNT-A (2 U per sciatic nerve) was administered in combination with BoNT-A-neutralising antitoxin (5 iu, i.t., 24 h post BoNT-A), and the immunoreactivity of BoNT-A-cleaved synaptosomal associated protein 25 (cSNAP-25) was examined on day 78 post BoNT-A. Fluorescent microphotographs show A.) BoNT-A enzymatic activity in neuromuscular junctions, terminals and axons in gastrocnemius (scale bar = 200 µm) and B.) L4 spinal cord ventral horn (upper panel scale bar = 500 µm, lower panel scale bar = 200 µm). Immunohistochemical scoring of muscular toxin activity C.) suggests abundant presence of cSNAP-25 in BoNT-A i.n. treated groups and positive controls (assessed 7 days post 5 U kg^{-1} i.m. BoNT-A). Under C.), the data points represent individual animal score values and the horizontal bar represents median (*N* = 3 animals/group). The cSNAP-25 quantity in the spinal cord ventral horn D.), assessed by sum of pixel intensity-thresholded area in 6 non-overlapping visual fields (0.14 mm2, 3 visual fields per left and right side; average of 4 slices per animals, *N* = 5 animals/group; median ± range, **P < 0.01 vs. saline i.n. + horse serum; Kruskal–Wallis followed by Dunn's post hoc).

Figure 8. Localization of BoNT-A enzymatic activity in relation to different neuronal and synaptic markers. The animals were treated with i.n. BoNT-A (2 U per bilateral sciatic nerve) and the L4 ventral horn sections were co-stained with BoNT-A-cleaved SNAP-25 immunoreactivity (cSNAP-25) and A.) choline acetyltransferase (ChAT), B.), potassium voltage channel $K_v2.1$., both markers of cholinergic C-boutons and their associated postsynaptic channels. In addition, colocalization of cSNAP-25 was performed with C.) high affinity BoNT-A binding acceptor synaptic vesicle protein 2 C (SV2C), and D.) general synaptic marker synaptophysin. The confocal microscope images represent a single optical slice (0.42 μm thickness), representative from at least 3 different animals injected with i.n. BoNT-A + horse serum (blue arrows indicate overlap of the immunoreactivities suggestive of colocalization, scale bars = 20 μm).

Figure 9. Schematic representation of some possible TeNT and BoNT-A actions in the spinal cord ventral horn. After its axonal transport and transcytosis, TeNT blocks inhibitory transmission by 1.) Renshaw cells, 2.) Ia inhibitory interneurons, as well as 3.) other types of inhibitory interneurons (glycinergic, GABA-ergic) not shown here for simplicity (Weise et al., 2019; Antonucci et al., 2008). When injected in sciatic nerve peripherally, BoNT-A is transported by anterograde axonal transport to muscle (where it's effect on presynaptic neuromuscular terminal of ACh exocytosis results in neuromuscular terminal silencing) and by retrograde axonal transport to central nervous system, where transcytosed BoNT-A may block the excitatory transmission by 4.) C-boutons formed by V0c cholinergic interneurons (Caleo and Mazzocchio, 2018), and 5.) other types of excitatory neurons (e.g. glutamatergic), in line with its selectivity for excitatory transmission (Restani et al., 2011). Possible BoNT-A central action at 6.) motoneuron recurrent axonal collaterals synapsing with Renshaw cells (Ramirez-Castaneda et al., 2013; Mazzocchio and Caleo, 2015) does not necessitate transcytosis. The figure was created with Biorender.com (accessed on 14/08/2023).

SUPPLEMENTARY FIGURE LEGEND

Supplementary figure S1. Representative images of immunohistochemical scoring system for presence of cSNAP-25 in neuromuscular junctions (NMJ) and axons, similar to Perier et al., 2021. Score 4 = the strong staining of frequent NMJs, terminals and intramuscular nerves (no. of axons ≥ 10), score 3 = the strong staining of frequent NMJ and nerve terminals; score 2 = the moderate staining of frequent NMJs; score 1 was assigned when only a few or weak NMJ staining was observed. Score 0 was given if there was no staining of NMJ, no staining of nerve terminal and no staining of axons.

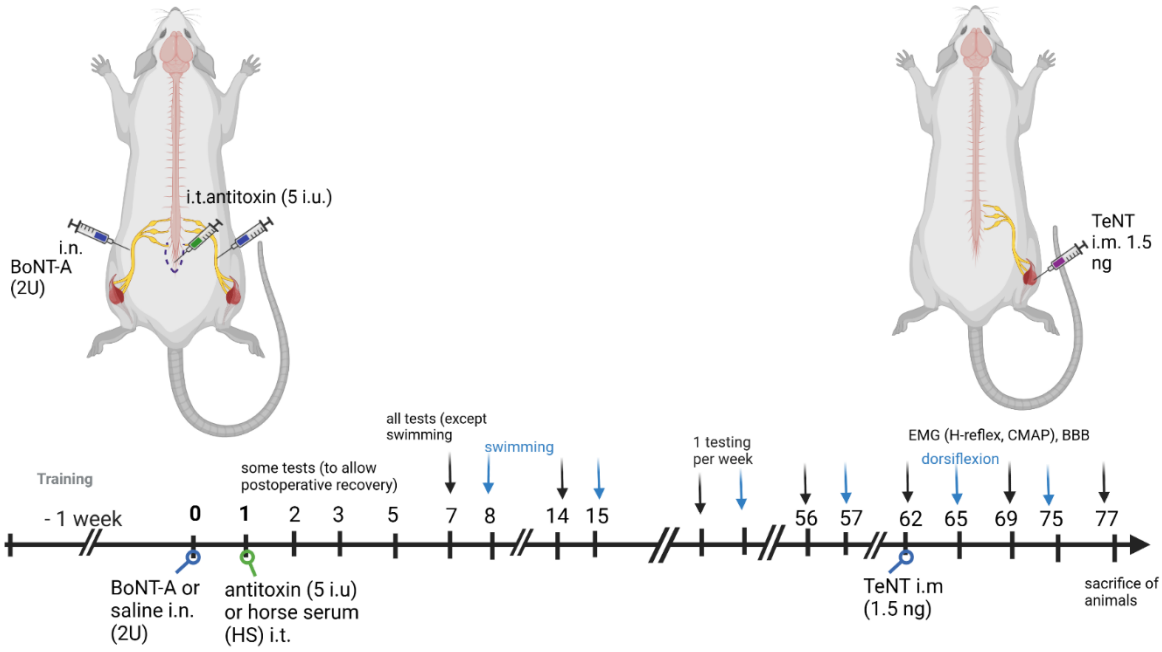
i.t.antitoxin (5 i.u.)
i.n.
BoNT-A
(2U)
TeNT
i.m. 1.5
ng
all tests (except
swimming
swimming
1 testing
per week
EMG (H-reflex, CMAP), BBB
dorsiflexion
some tests (to allow
postoperative recovery)
Training
- 1 week
0
1
2
3
5
7
8
14
15
56
57
62
65
69
75
77
BoNT-A or
saline i.n.
(2U)
antitoxin (5 i.u)
or horse serum
(HS) i.t.
TeNT i.m
(1.5 ng)
sacrifice of
animals

Figure 1

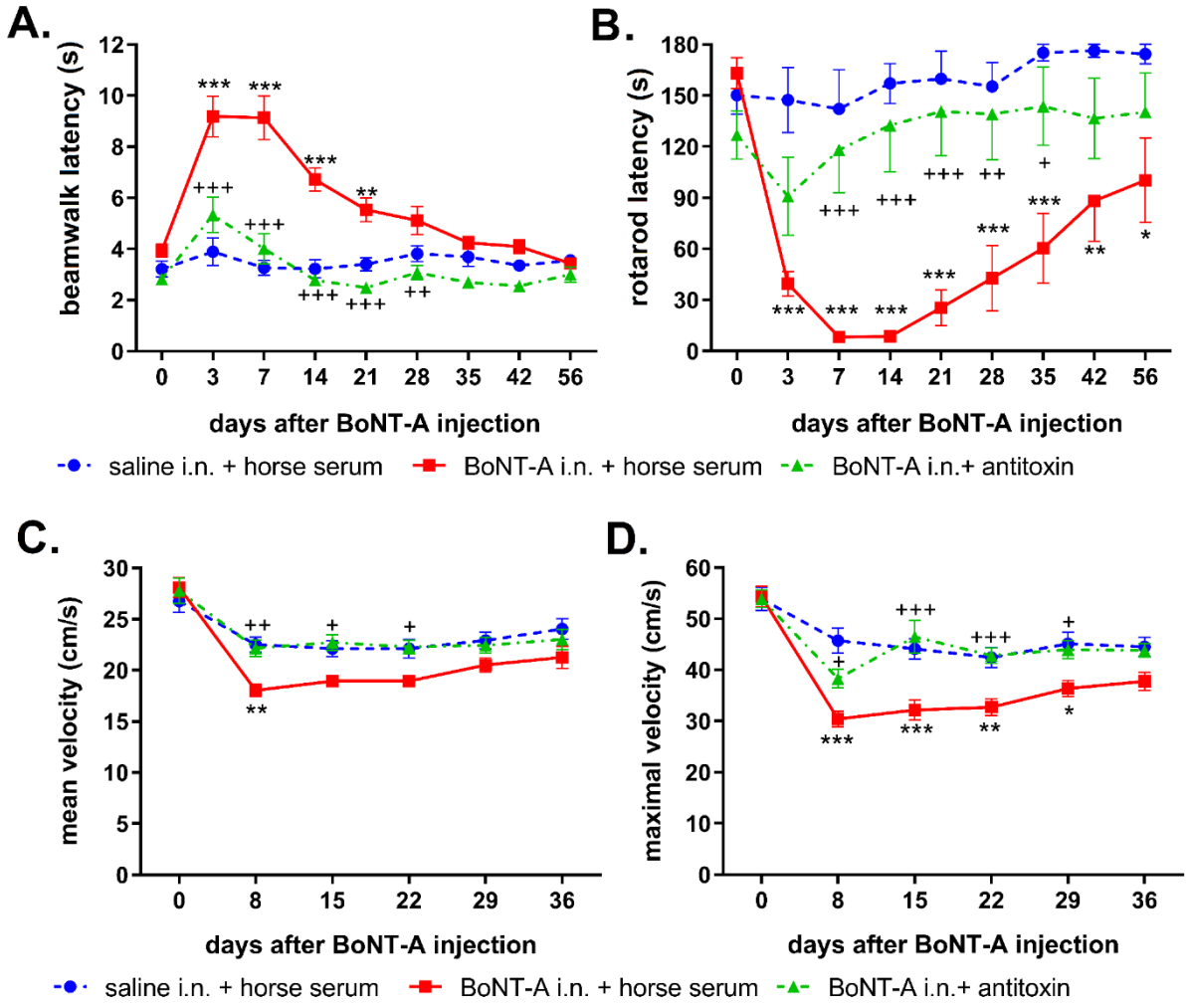
A.
beamwalk latency (s)
days after BoNT-A injection
B.
rotarod latency (s)
days after BoNT-A injection
saline i.n. + horse serum
BoNT-A i.n. + horse serum
BoNT-A i.n.+ antitoxin
C.
mean velocity (cm/s)
days after BoNT-A injection
D.
maximal velocity (cm/s)
days after BoNT-A injection
saline i.n. + horse serum
BoNT-A i.n. + horse serum
BoNT-A i.n.+ antitoxin

Figure 2

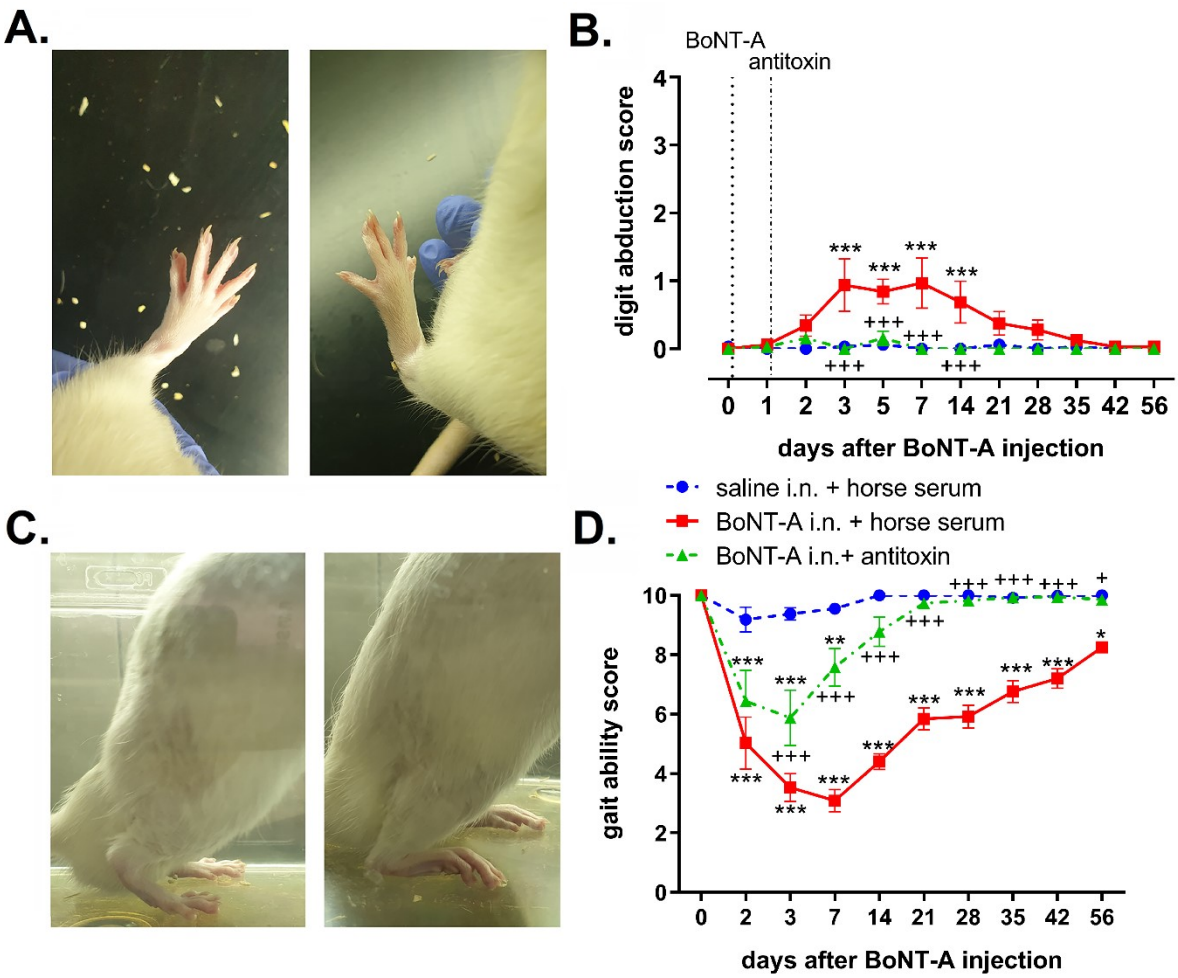
A.
B.
BoNT-A
antitoxin
digit abduction score
days after BoNT-A injection
C.
D.
saline i.n. + horse serum
BoNT-A i.n. + horse serum
BoNT-A i.n.+ antitoxin
gait ability score
days after BoNT-A injection

Figure 3

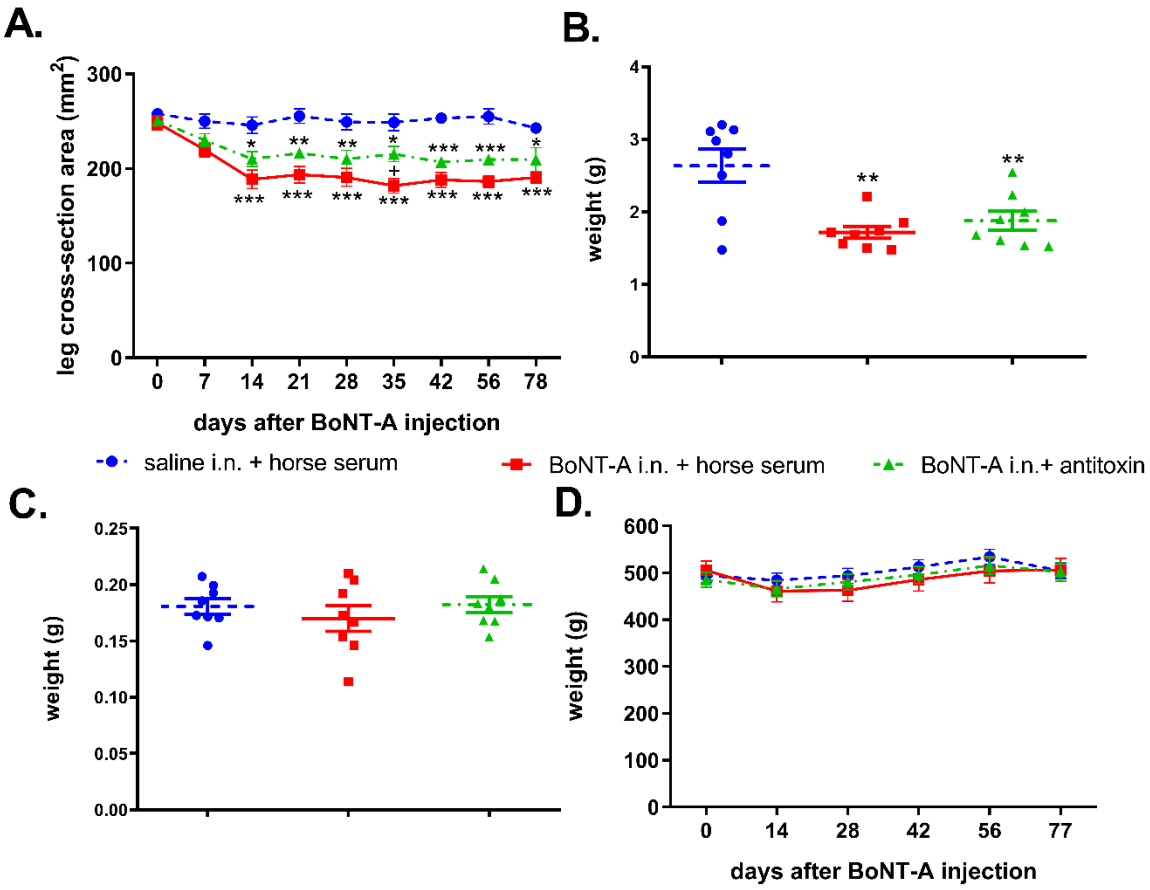
A.
B.
leg cross-section area (mm2)
300
200
100
0
0 7 14 21 28 35 42 56 78
days after BoNT-A injection
weight (g)
4
3
2
1
0
saline i.n. + horse serum
BoNT-A i.n. + horse serum
BoNT-A i.n.+ antitoxin
C.
D.
weight (g)
0.25
0.20
0.15
0.10
0.05
0.00
weight (g)
600
500
400
300
200
100
0
0 14 28 42 56 77
days after BoNT-A injection

Figure 4

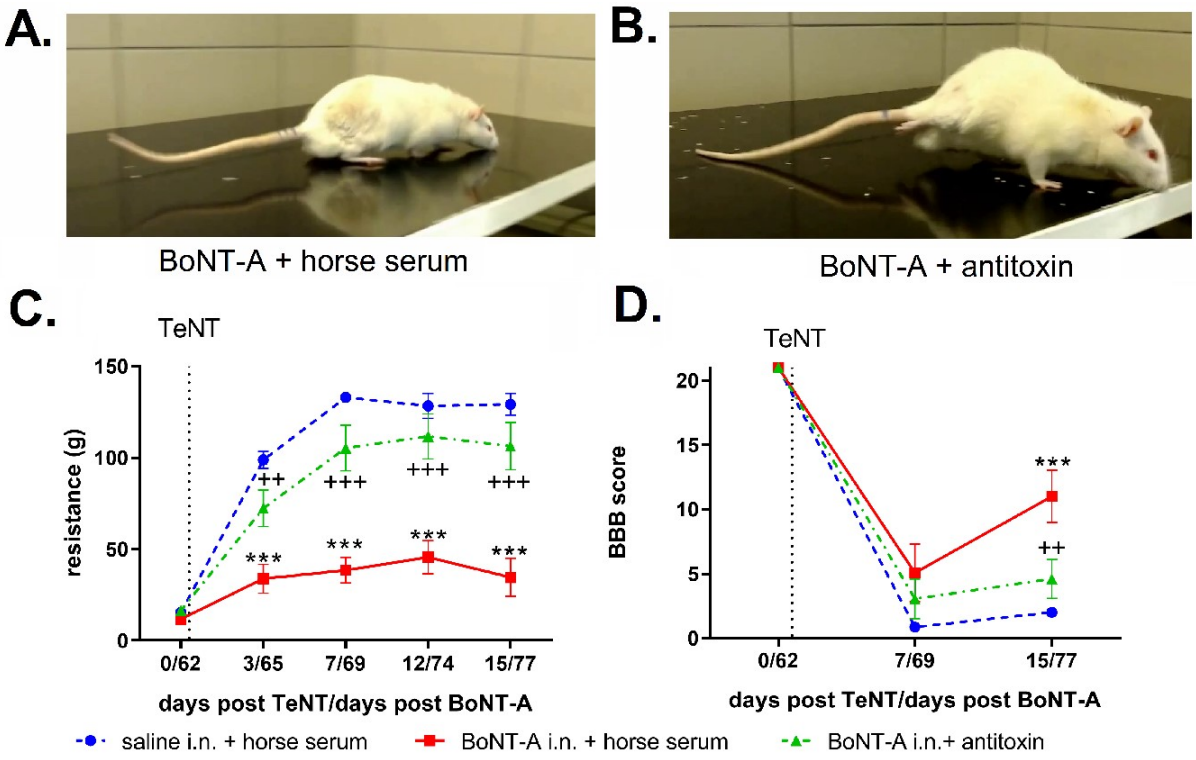
A.
B.
BoNT-A + horse serum
BoNT-A + antitoxin
C.
TeNT
resistance (g)
150
100
50
0
++
+++
+++
+++
***
***
***
***
0/62
3/65
7/69
12/74
15/77
days post TeNT/days post BoNT-A
D.
TeNT
BBB score
20
15
10
5
0
***
++
0/62
7/69
15/77
days post TeNT/days post BoNT-A
saline i.n. + horse serum
BoNT-A i.n. + horse serum
BoNT-A i.n.+ antitoxin

Figure 5

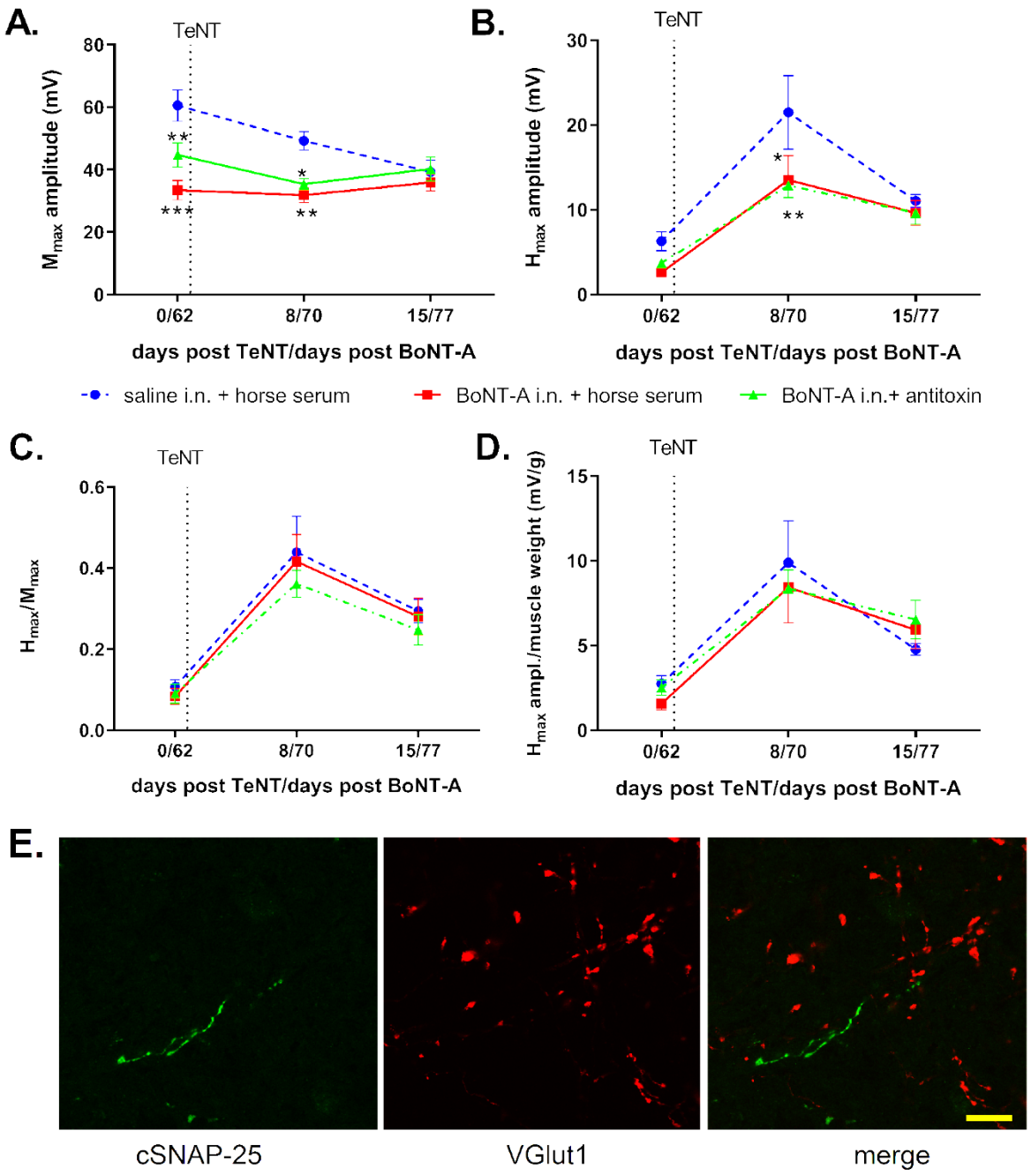
A.
TeNT
M_{max} amplitude (mV)
80
60
40
20
0
**
***
*
**
0/62
8/70
15/77
days post TeNT/days post BoNT-A
B.
TeNT
H_{max} amplitude (mV)
30
20
10
0
*
**
0/62
8/70
15/77
days post TeNT/days post BoNT-A
saline i.n. + horse serum
BoNT-A i.n. + horse serum
BoNT-A i.n.+ antitoxin
C.
TeNT
H_{max}/M_{max}
0.6
0.4
0.2
0.0
0/62
8/70
15/77
days post TeNT/days post BoNT-A
D.
TeNT
H_{max} ampl./muscle weight (mV/g)
15
10
5
0
0/62
8/70
15/77
days post TeNT/days post BoNT-A

E.
cSNAP-25
VGlut1
merge

Figure 6

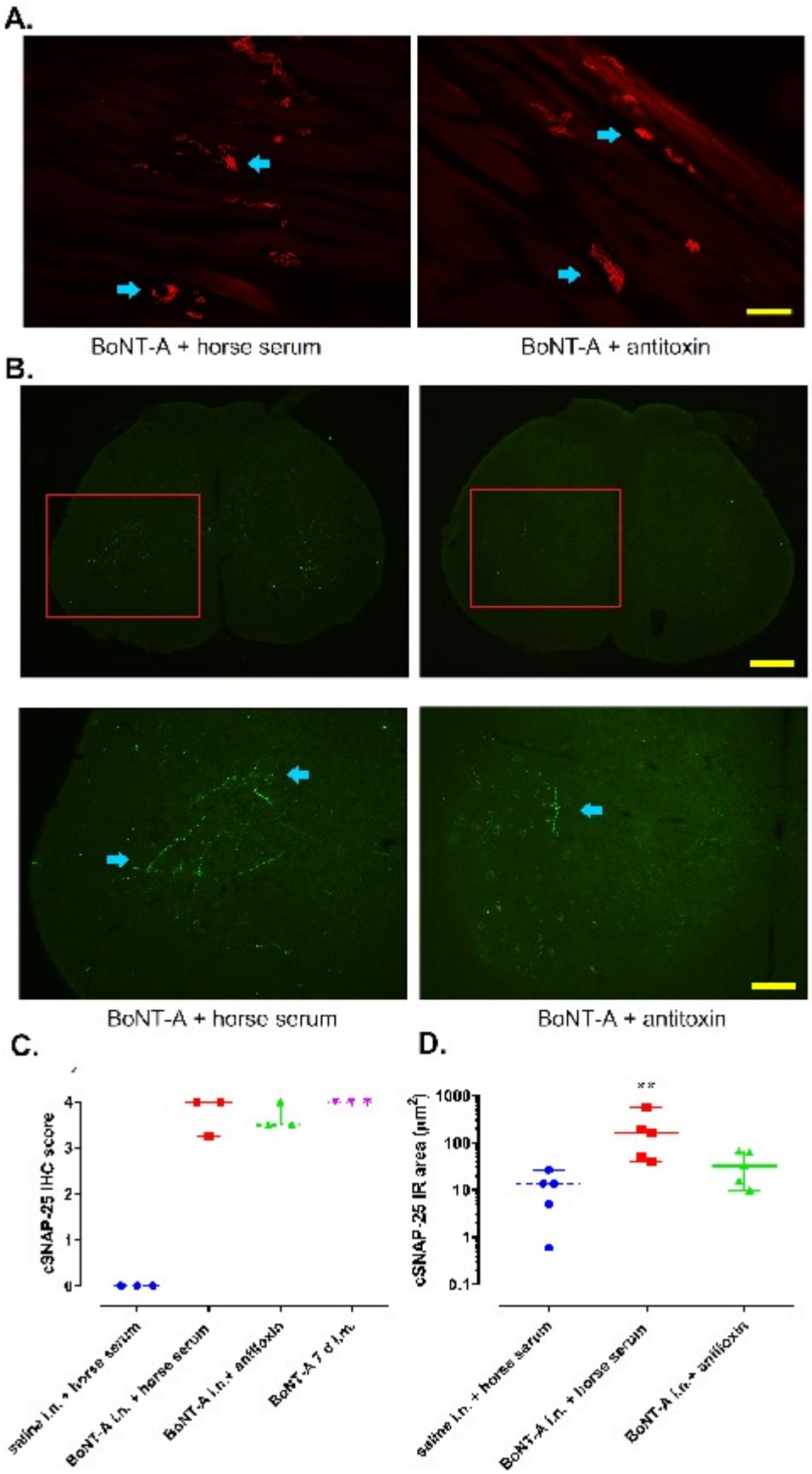
A.
BoNT-A + horse serum
BoNT-A + antitoxin
B.
BoNT-A + horse serum
BoNT-A + antitoxin
C.
cSNAP-25 IHC score
0
1
2
3
4
saline i.n. + horse serum
BoNT-A i.n. + horse serum
BoNT-A i.n.+ antitoxin
BoNT-A 7 d i.m.
D.
cSNAP-25 IR area (µm²)
0.1
1
10
100
1000
**
saline i.n. + horse serum
BoNT-A i.n. + horse serum
BoNT-A i.n.+ antitoxin

Figure 7

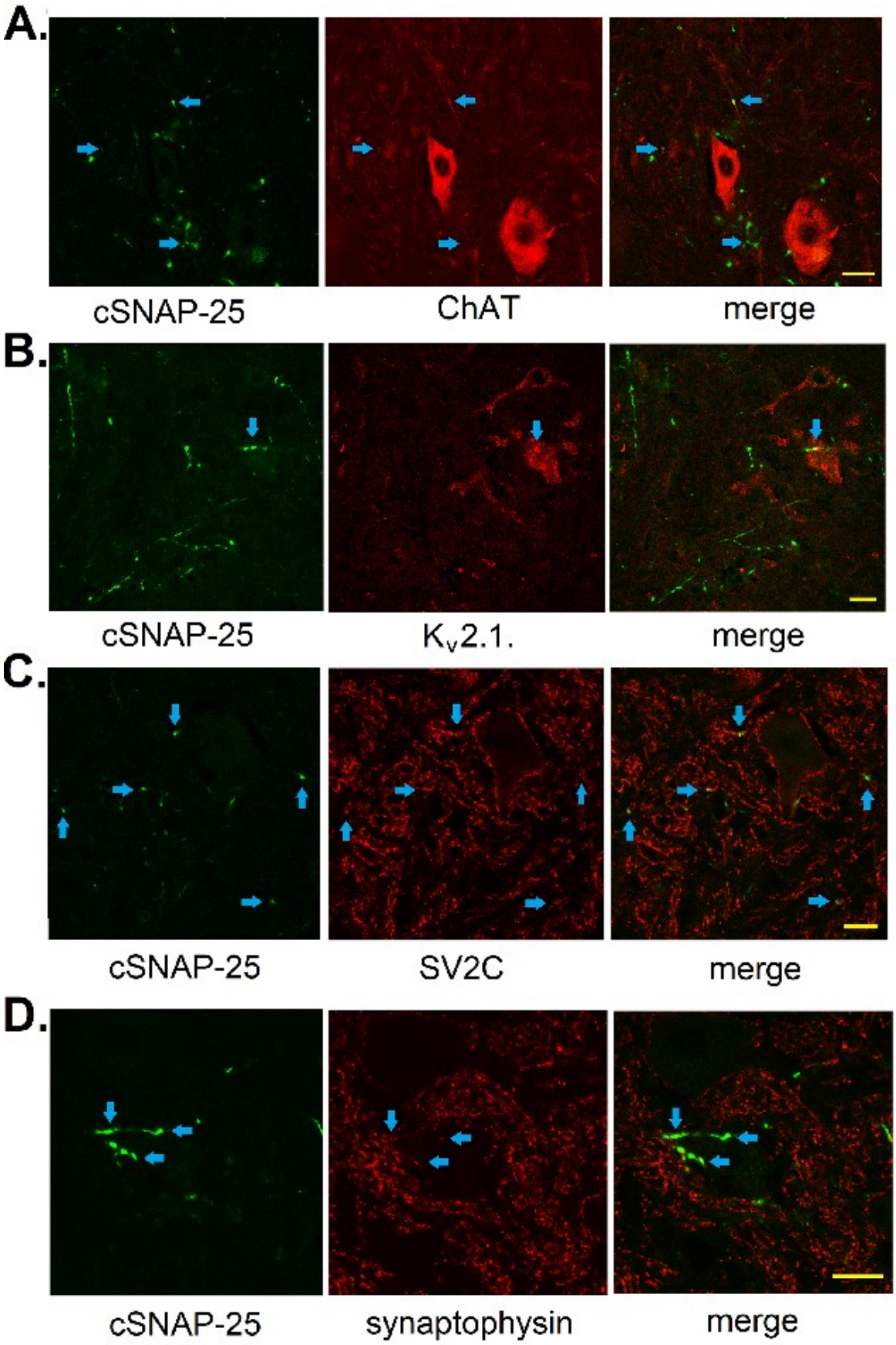
A.
cSNAP-25
ChAT
merge
B.
cSNAP-25
K_v2.1.
merge
C.
cSNAP-25
SV2C
merge
D.
cSNAP-25
synaptophysin
merge

Figure 8

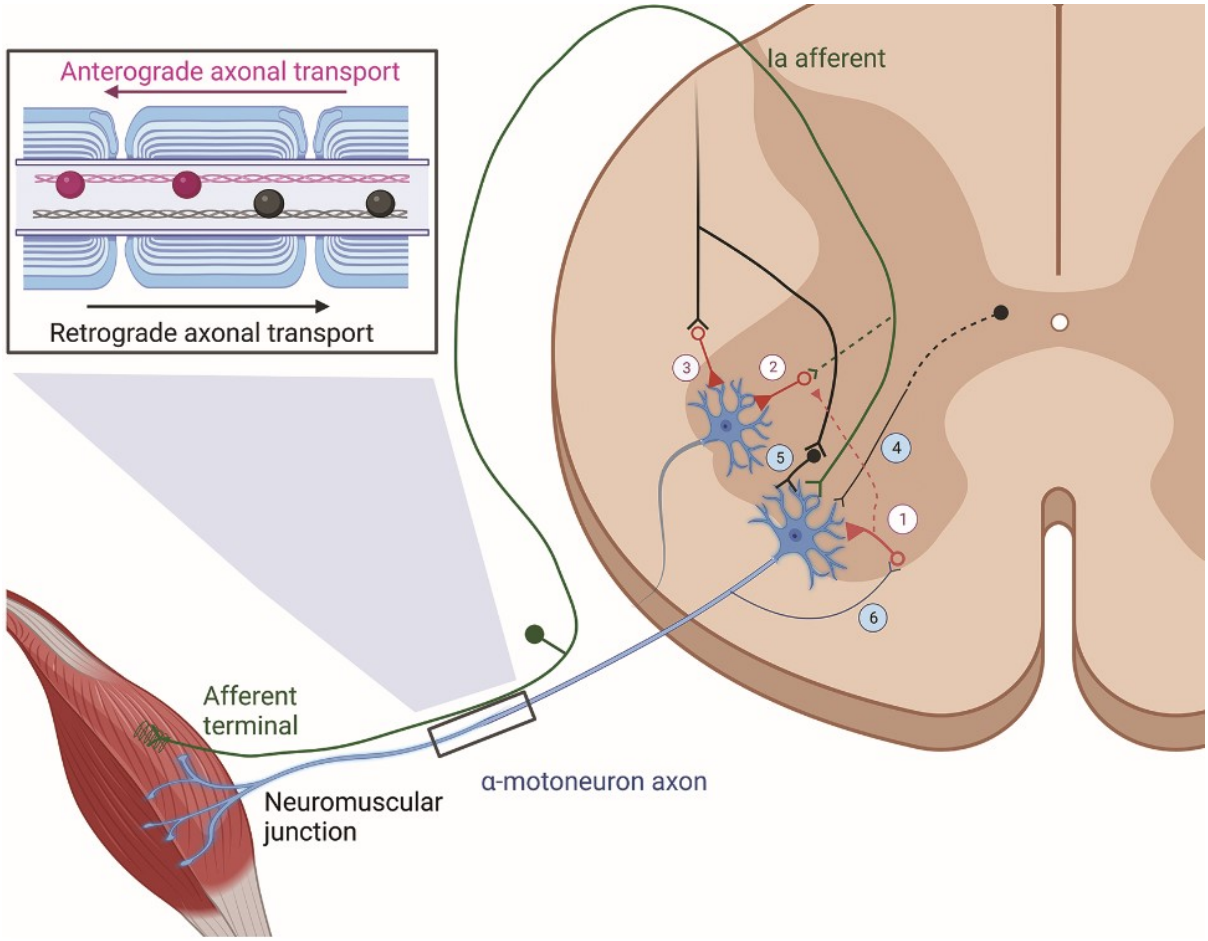
Anterograde axonal transport
Retrograde axonal transport
Ia afferent
3
2
5
4
1
6
Afferent
terminal
α-motoneuron axon
Neuromuscular
junction

Figure 9

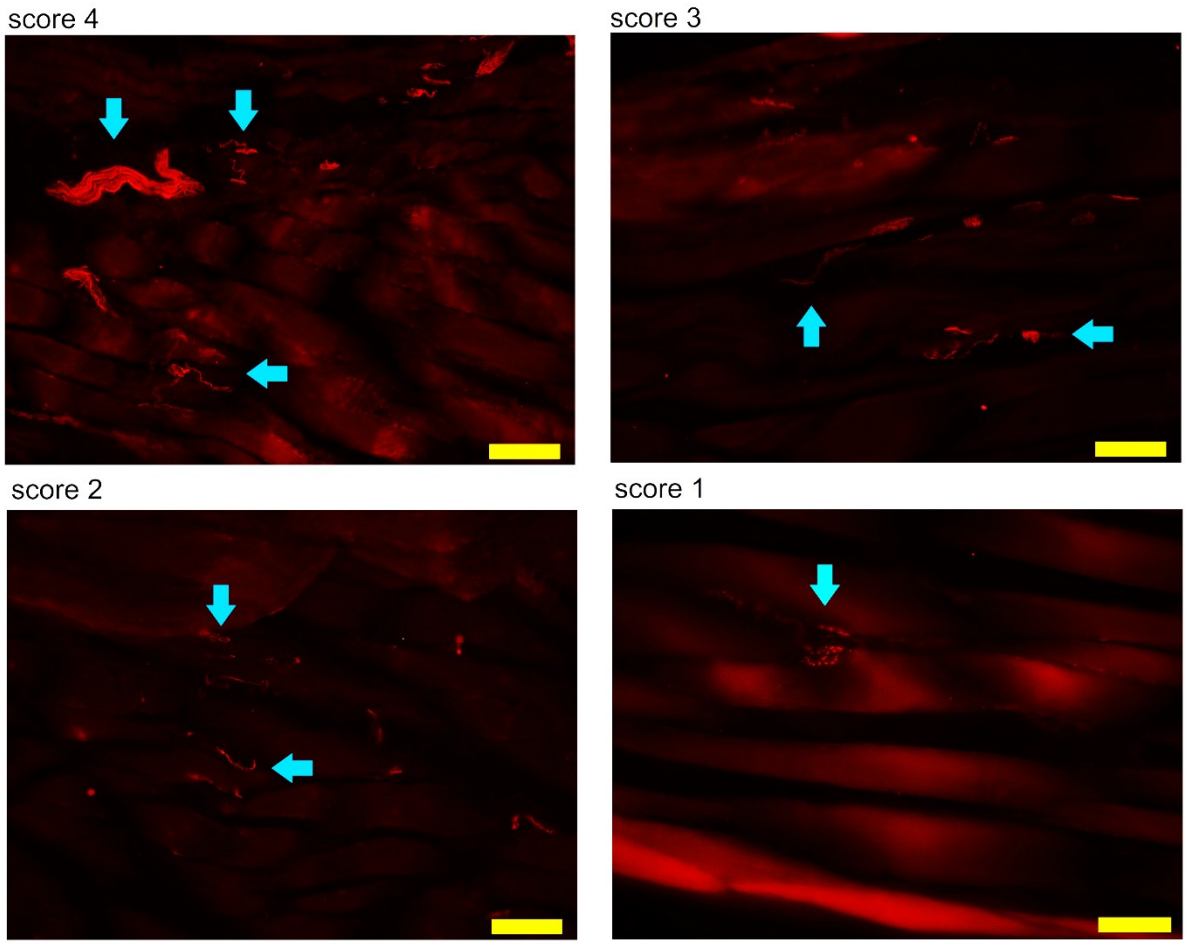

Supplementary Figure S1